– **Typeset by GMNI &** FoilTeX –

A HIGH-ORDER CHIMERA METHOD BASED ON MOVING LEAST SQUARES

L. Ramírez[a], X. Nogueira[a], P. Ouro[b], F. Navarrina[a], I. Colominas[a]

a: Dept. of Applied Mathematics
Civil Engineering School
University of A Coruña, Spain

Hydro-Environmental Research Centre
School of Engineering
Cardiff University

e-mail: luis.ramirez@udc.es
web page: http://caminos.udc.es/gmni

Outline

- Introduction
- The FV-MLS method
- A MLS-based sliding mesh technique
- A High-order Chimera method
- An immersed boundary method for unstructured meshes
- Conclusions

Outline

- Introduction
- The FV-MLS method
- A MLS-based sliding mesh technique
- A High-order Chimera method
- An immersed boundary method for unstructured meshes
- Conclusions

Introduction

- Origin of this research:
  - Development of more accurate numerical methods for complex geometries and moving boundaries.
  - Standard industrial codes: 2^{nd} order.
  - We need high-resolution schemes for unstructured grids.
  - Turbomachinery $\Rightarrow$ Relative motion rotor/stator.

Introduction

- It is not straightforward to obtain finite volume methods with order higher than two on unstructured grids.
- One of the main difficulties is the computation of high-order derivatives.

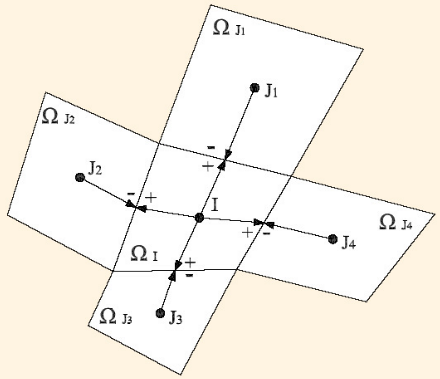

Outline

- Introduction
- The FV-MLS method
- A MLS-based sliding mesh technique
- A High-order Chimera method
- An immersed boundary method for unstructured meshes
- Conclusions

The MLS method in a nutshell

- MLS is an approximation method very used by the meshless community.
- MLS performs a reconstruction of $\mathrm{u}(\boldsymbol{x})$ at a point $\boldsymbol{x}$ by using a weighted LS approximation in the vicinity of $\boldsymbol{x}$.
- The approximation is written in terms of MLS shape functions.

$$\boxed{\hat{u}(\boldsymbol{x}) = \sum_{j=1}^{n_{\mathrm{x}}} N_j(\boldsymbol{x}) u_j}$$

- The approximation basically depends on a kernel and a basis function.

Kernel functions

- Many functions used as kernels: splines, gaussians
- An example, the cubic spline:

$$W_j(\boldsymbol{x}) = W(\boldsymbol{x}-\boldsymbol{x}_j, h) = \frac{\alpha}{h^\nu}\begin{cases} 1-\frac{3}{2}s^2+\frac{3}{4}s^3 & s \leq 1 \\ \frac{1}{4}(2-s)^3 & 1 < s \leq 2 \\ 0 & s > 2 \end{cases}$$

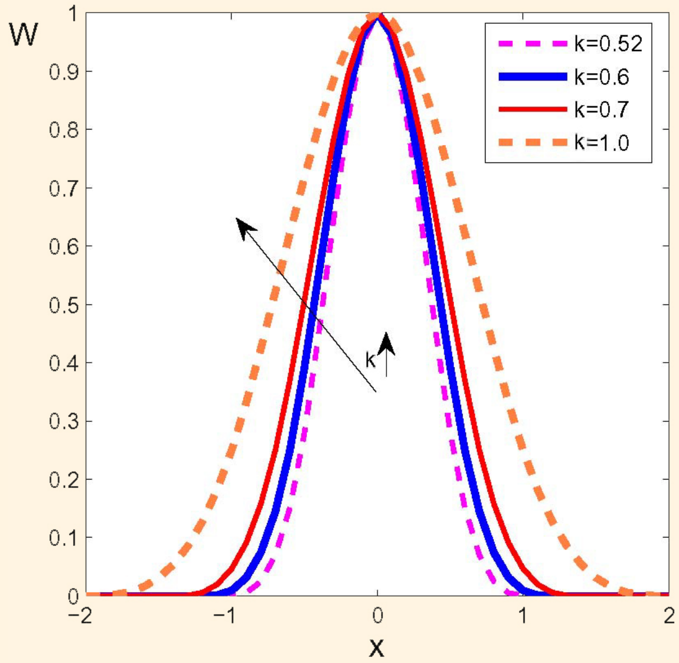

$$s = \frac{\|\boldsymbol{x}-\boldsymbol{x}_j\|}{h}$$

$$h = k \max\left(\|\boldsymbol{x}-\boldsymbol{x}_j\|\right)$$

Kernel functions

- Many functions used as kernels: splines, gaussians
- An example, the cubic spline:

$$W_j(\boldsymbol{x}) = W(\boldsymbol{x}-\boldsymbol{x}_j, h) = \frac{\alpha}{h^\nu}\begin{cases} 1-\frac{3}{2}s^2+\frac{3}{4}s^3 & s \leq 1 \\ \frac{1}{4}(2-s)^3 & 1 < s \leq 2 \\ 0 & s > 2 \end{cases}$$

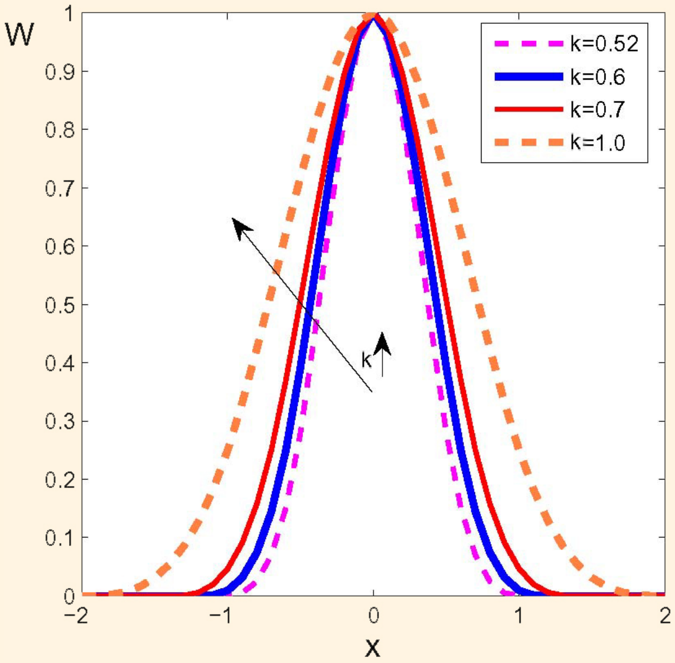

$$s = \frac{\|\boldsymbol{x}-\boldsymbol{x}_j\|}{h}$$

$$h = \boldsymbol{k}\max\left(\|\boldsymbol{x}-\boldsymbol{x}_j\|\right)$$

Kernel functions

- Another example: Exponential Kernel.

$$W(x,x^*,\kappa) = \frac{e^{-\left(\frac{s}{c}\right)^2} - e^{-\left(\frac{dm}{c}\right)^2}}{1 - e^{-\left(\frac{dm}{c}\right)^2}}$$

$$s = |x - x^*|\,, d_m = 2\max\left(|x_j - x^*|\right), c = \frac{d_m}{2\kappa}$$

- A 2D kernel is obtained by multiplying two 1D kernels:

$$W_j(\boldsymbol{x},\boldsymbol{x}^*,\kappa_x,\kappa_y) = W_j(x,x^*,\kappa_x)W_j(y,y^*,\kappa_y)$$

- Another example: Exponential Kernel.

$$W(x, x^*, \boldsymbol{\kappa}) = \frac{e^{-\left(\frac{s}{c}\right)^2} - e^{-\left(\frac{dm}{c}\right)^2}}{1 - e^{-\left(\frac{dm}{c}\right)^2}}$$

$$s = \left|x - x^*\right|, d_m = 2\max\left(\left|x_j - x^*\right|\right), c = \frac{d_m}{2\boldsymbol{\kappa}}$$

- A 2D kernel is obtained by multiplying two 1D kernels:

$$W_j(\boldsymbol{x}, \boldsymbol{x}^*, \kappa_x, \kappa_y) = W_j(x, x^*, \kappa_x)W_j(y, y^*, \kappa_y)$$

Kernel functions

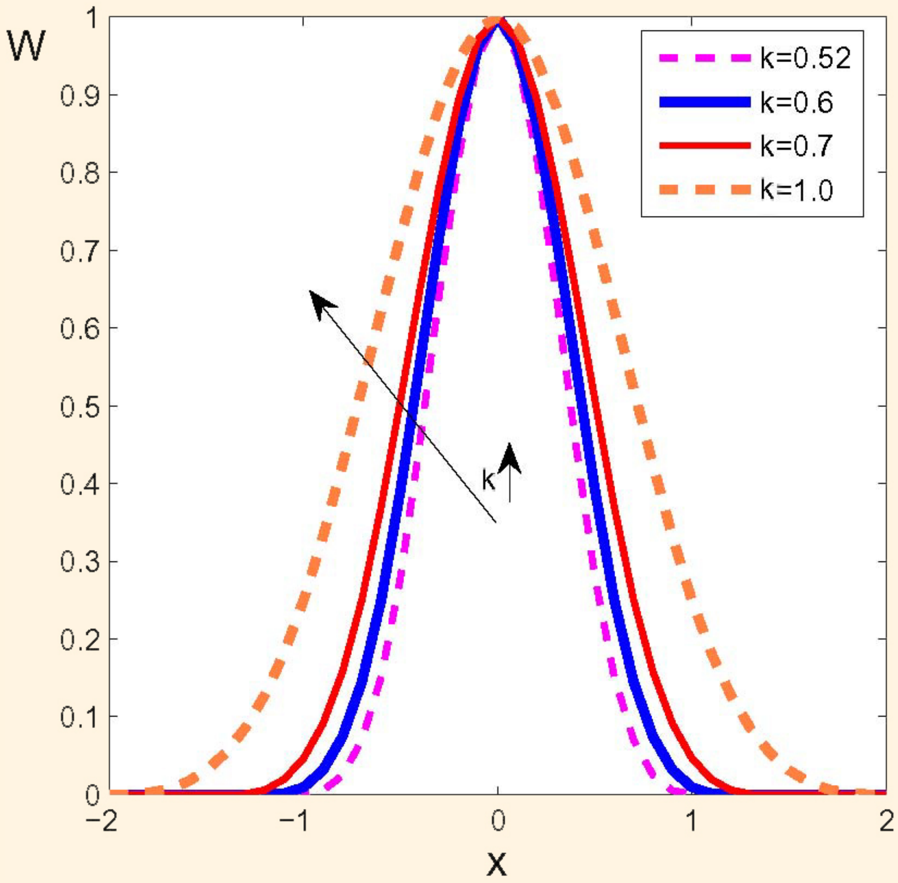

CUBIC SPLINE

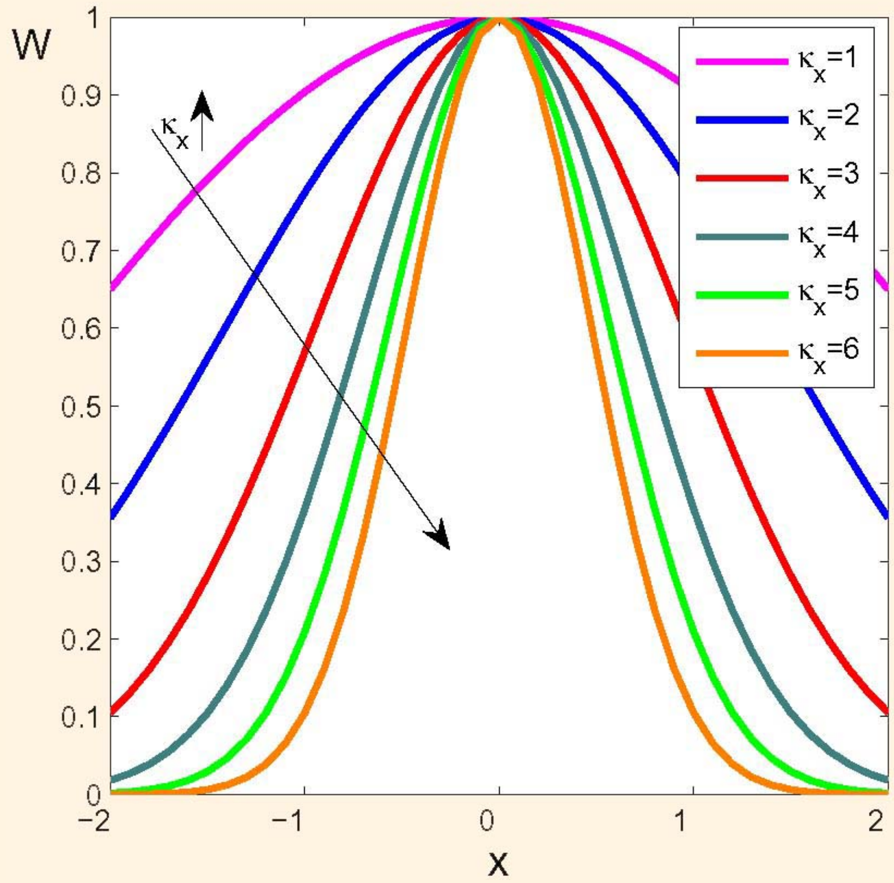

EXPONENTIAL KERNEL

A practical note

- Vertices and/or centroids of the control cells are the "particles" to perform the MLS approximation.
- We need to define stencils to "mark" the neighbor particles that define the cloud of points.

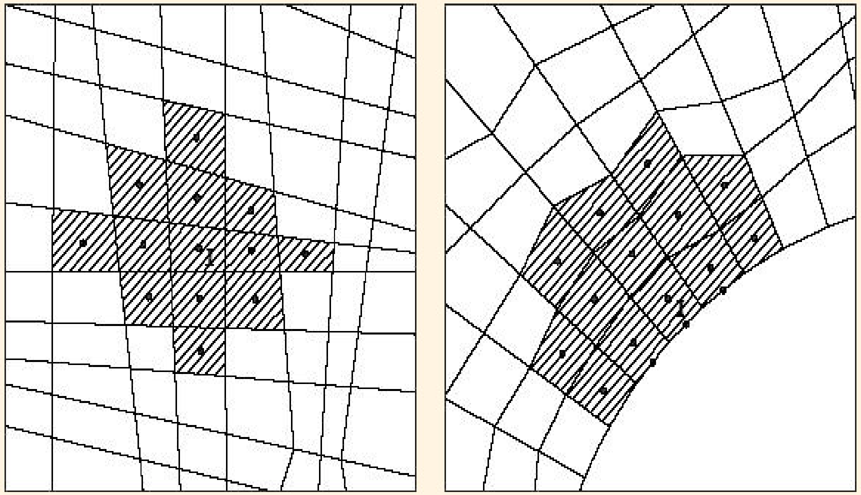

- We use a polynomial cubic basis in all the computations.

The FV-MLS method

- In order to develop high-order finite volume schemes:
  - Compute fluxes more accurately.
  - Improve function reconstruction at an integration point $\boldsymbol{x}$ placed at the interface between elements.

$$\boldsymbol{U}(x) = \boldsymbol{U_I} + \nabla \boldsymbol{U_I} \cdot (\boldsymbol{x} - \boldsymbol{x_I}) + \frac{1}{2}(\boldsymbol{x} - \boldsymbol{x_I})^T \boldsymbol{H_I}(\boldsymbol{x} - \boldsymbol{x_I}) + \ldots$$

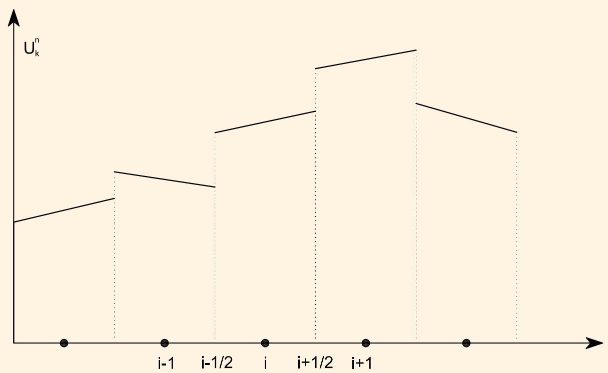

Piece-wise linear reconstruction of a function.

The FV-MLS method

- Computation of high-order derivatives:
  - Easy on structured grids.
  - Unstructured grids $\Rightarrow$ PROBLEM.

- We propose:
  - The use of Moving Least Squares (MLS) to obtain an accurate and multidimensional approximation of derivatives on unstructured grids.

The FV-MLS method

- This scheme acknowledge the different nature of convective and diffusive terms.
- We start from a high-order, continuous MLS approximation of the solution:
- Convective terms discretization:
  - Breaks the continuous representation of the MLS approximation.
  - Obtains a continuous representation of the variables inside each cell.
- Diffusive terms discretization is:
  - Centered.
  - Continuous.
  - Highly accurate.

A MLS-based sliding mesh technique

- Introduction
- The FV-MLS method
- A MLS-based sliding mesh technique
- A High-order Chimera method
- An immersed boundary method for unstructured meshes
- Conclusions

Wind turbine

Engine fan

A MLS based sliding-mesh technique

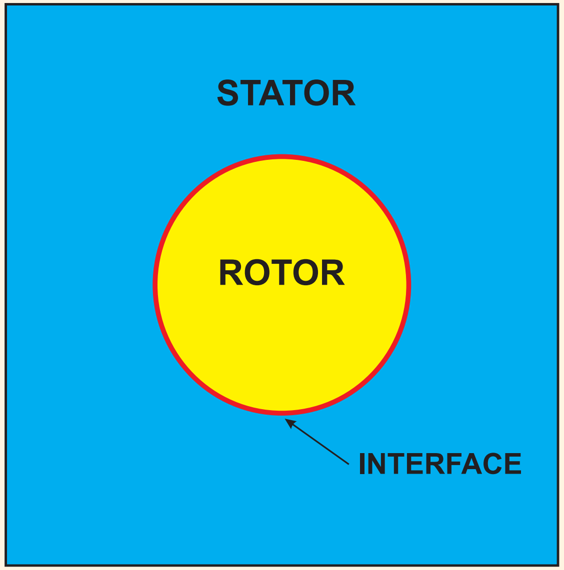

- Two different approaches
  - 1. MLS-based sliding mesh with intersections.
  - 2. Interface halo-cell sliding mesh.

MLS-based sliding mesh with intersections

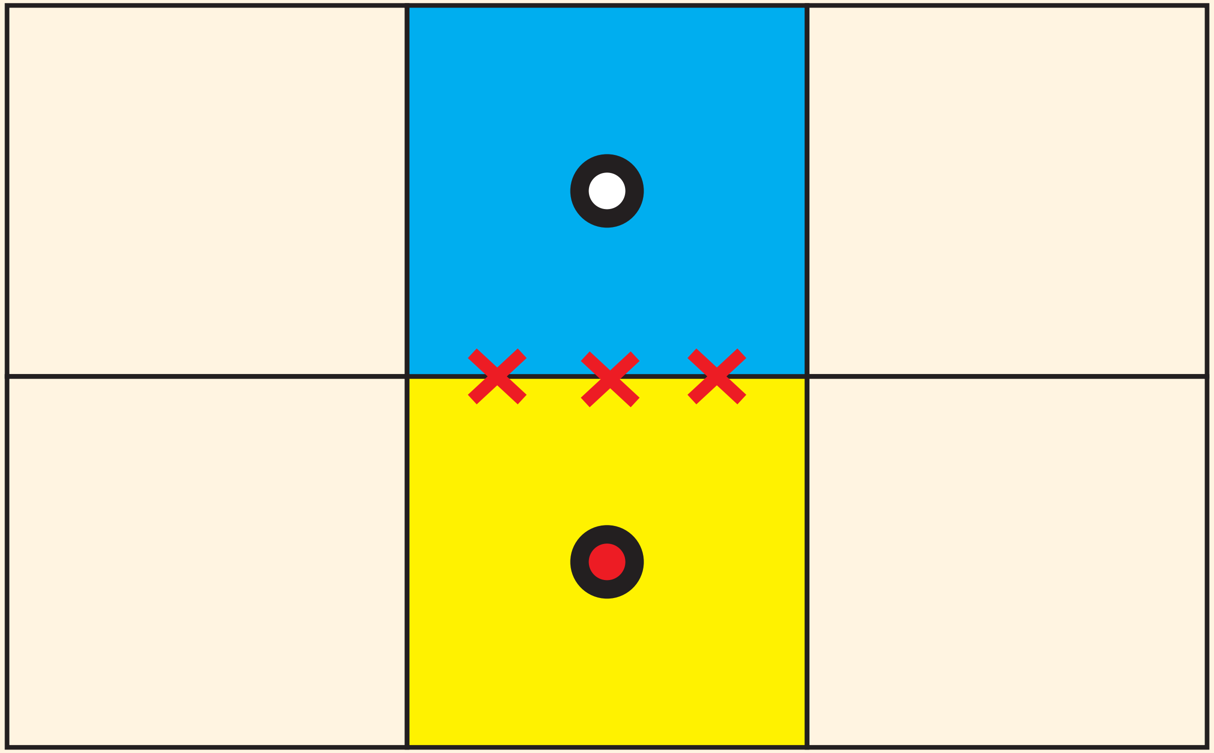

MLS-based sliding mesh with intersections

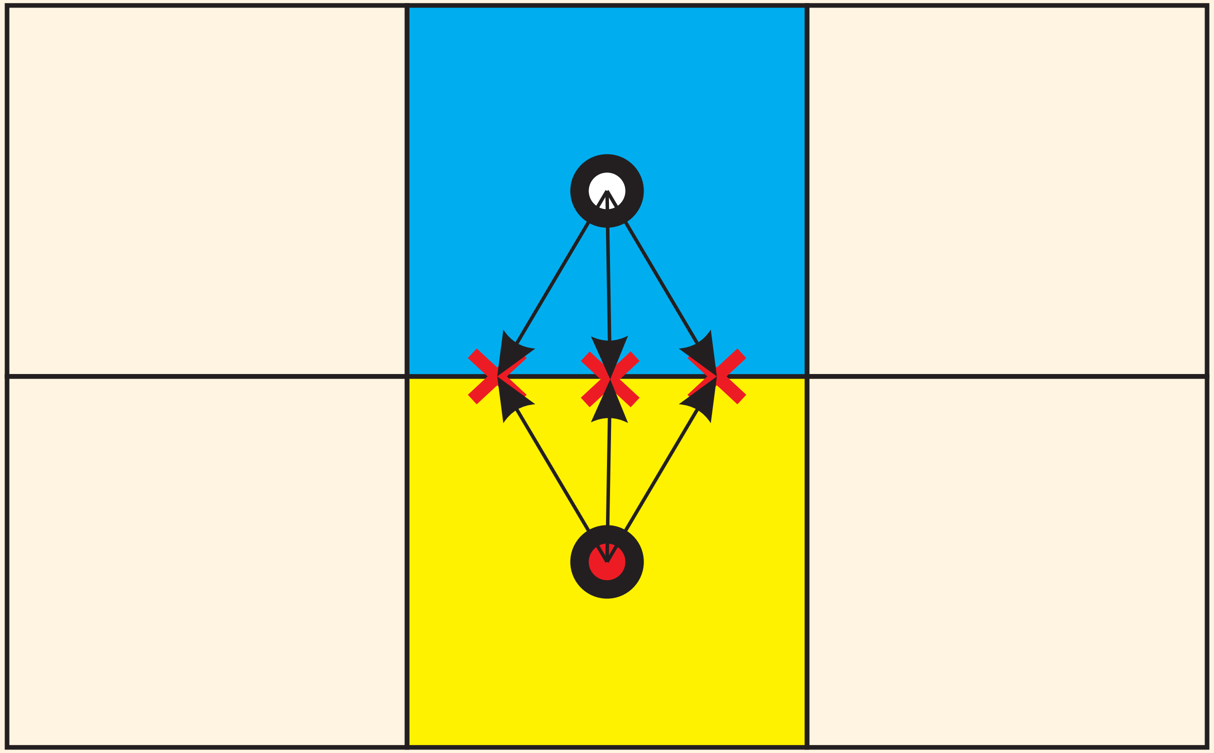

MLS-based sliding mesh with intersections

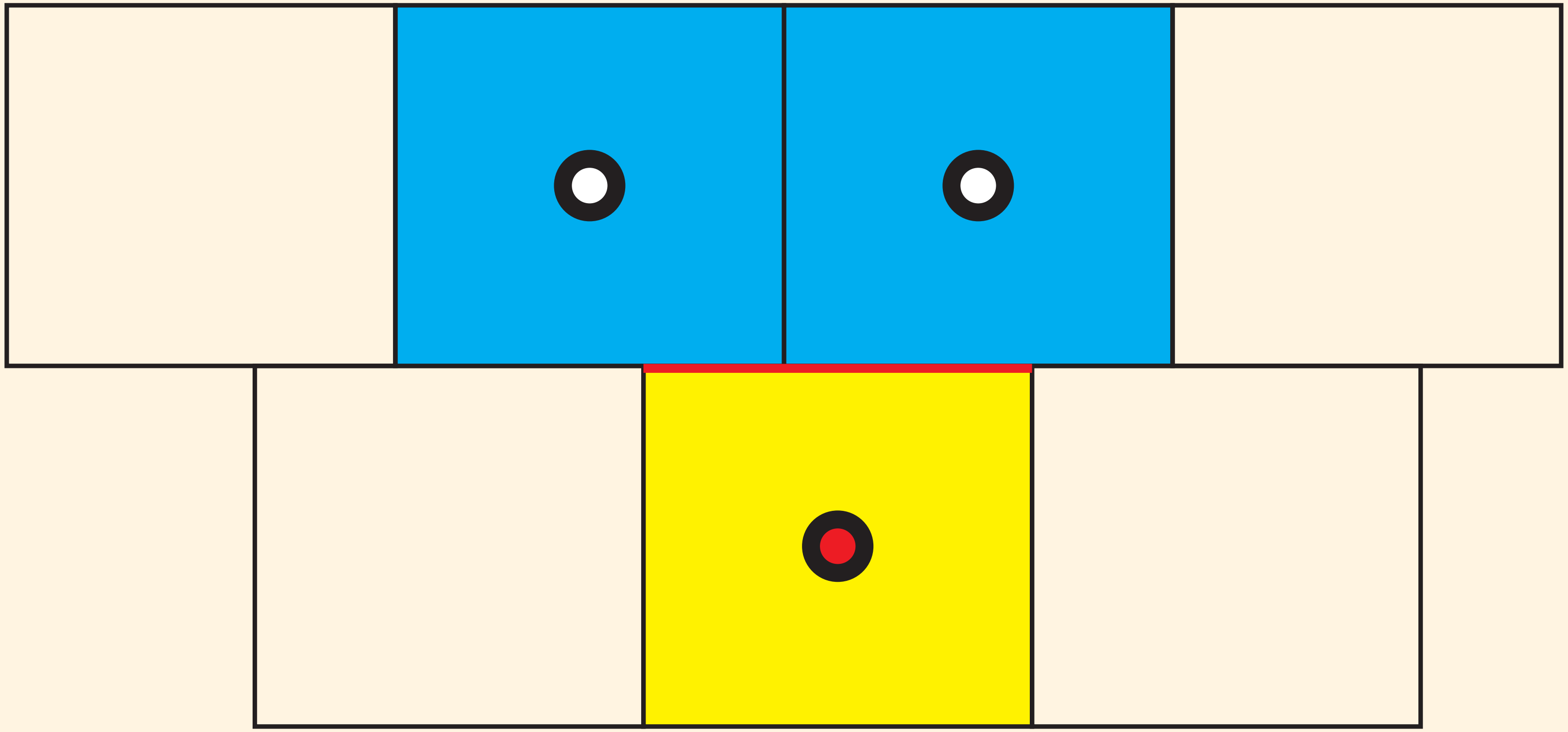

MLS-based sliding mesh with intersections

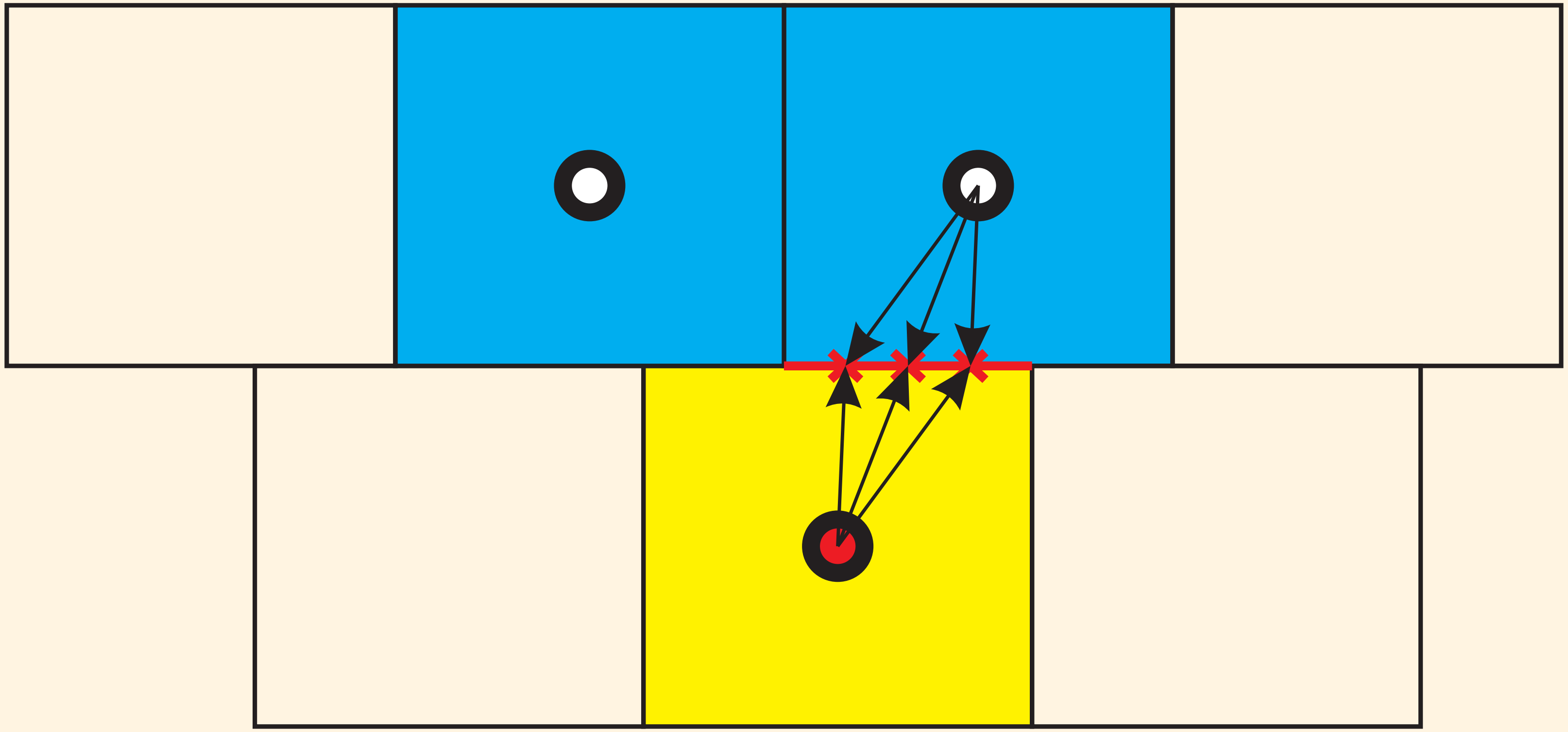

MLS-based sliding mesh with intersections

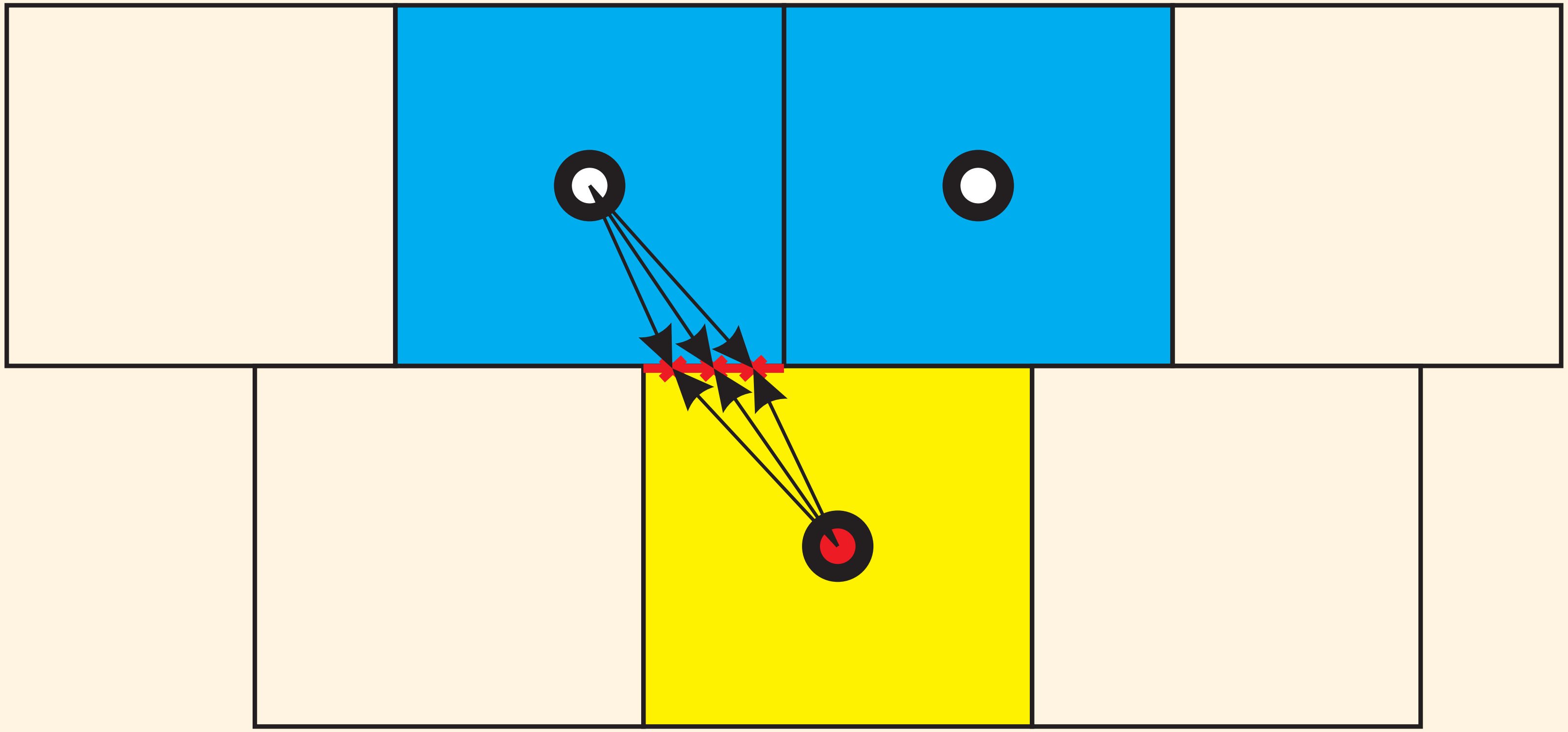

- MLS-based sliding mesh with intersections.
  - Recursive searching of intersection nodes.
  - Computation of the numerical flux at interface.

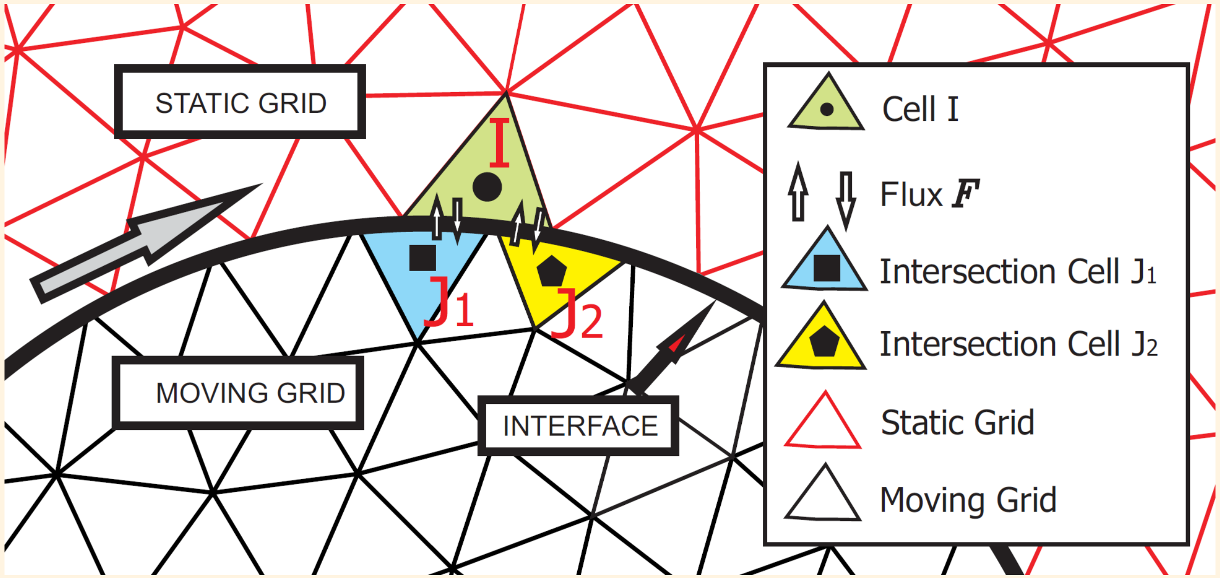

A MLS-based sliding mesh technique

- MLS-based sliding mesh with intersections.
  - The stencil can be defined as:

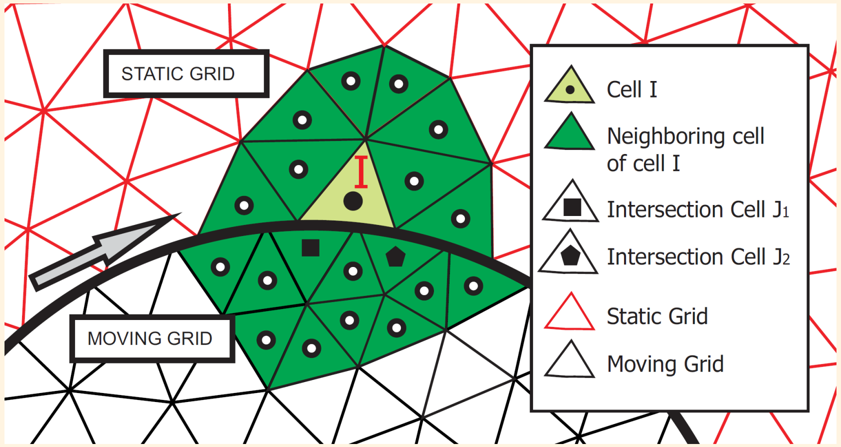

Full Stencil

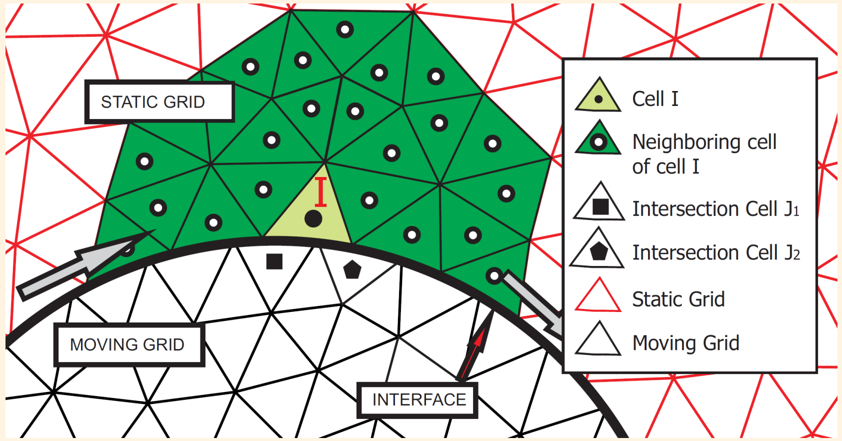

Half Stencil

A MLS-based sliding mesh technique

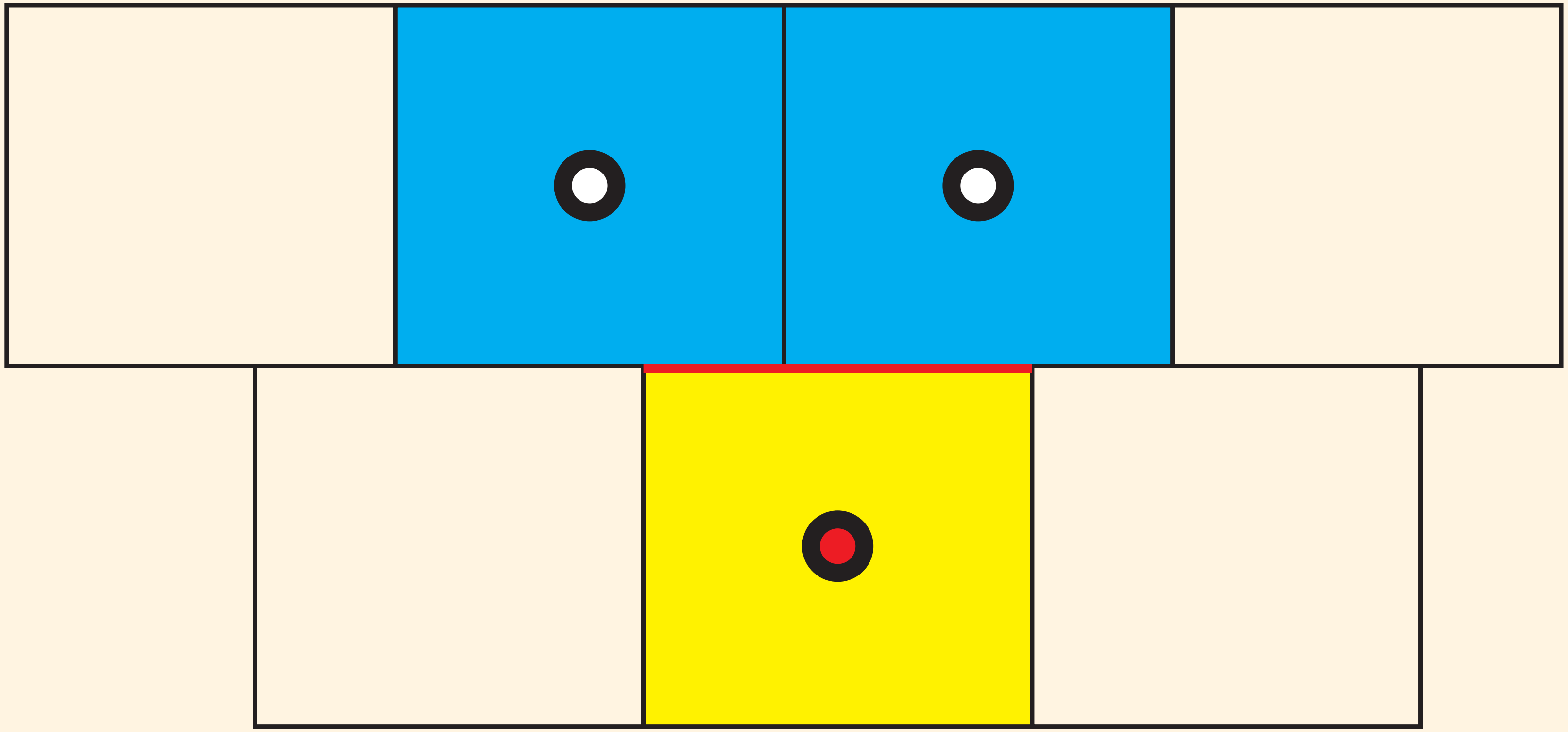

A MLS-based sliding mesh technique

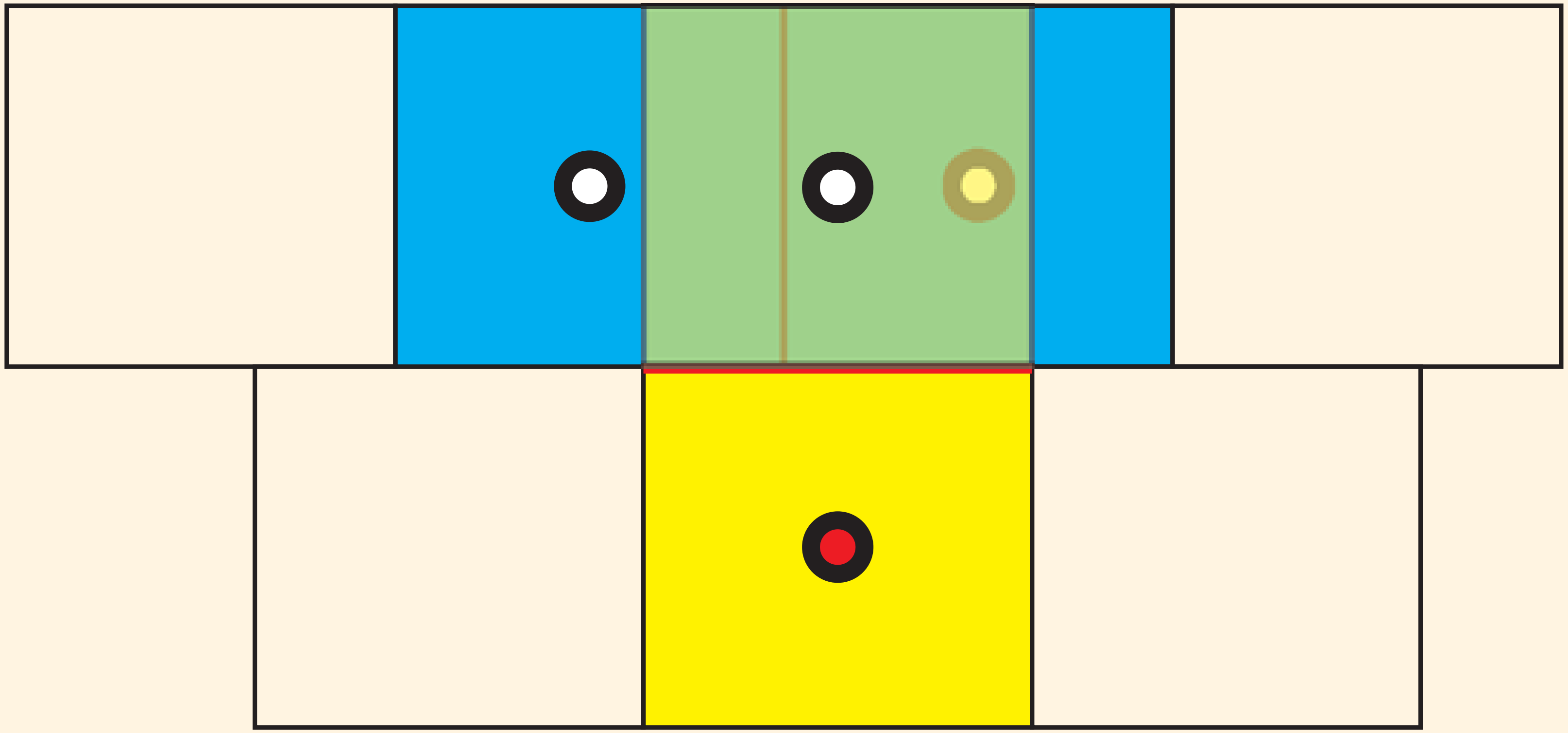

A MLS-based sliding mesh technique

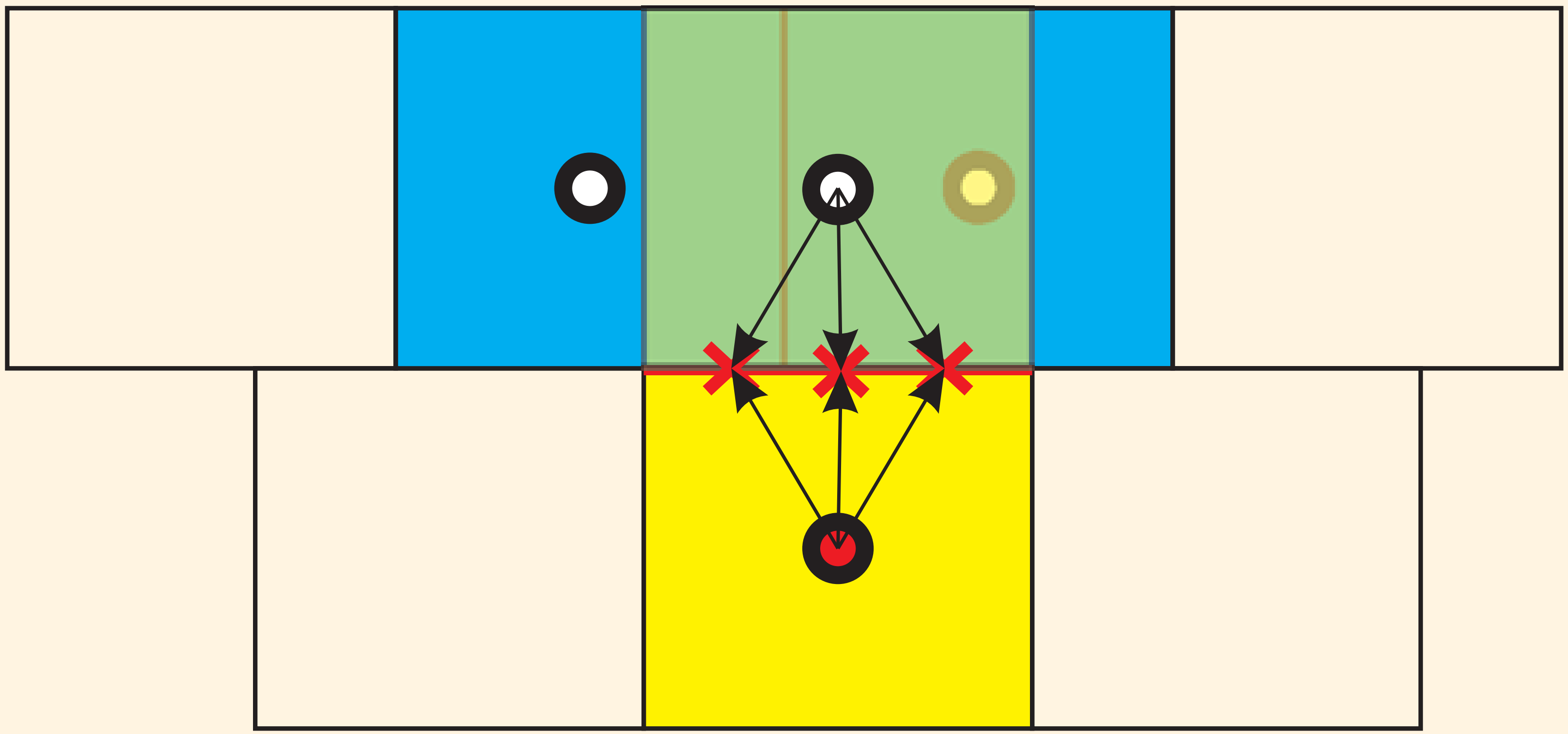

- Interface halo cell sliding mesh.
  - Create a halo cell.
  - Computation of the numerical flux at interface.

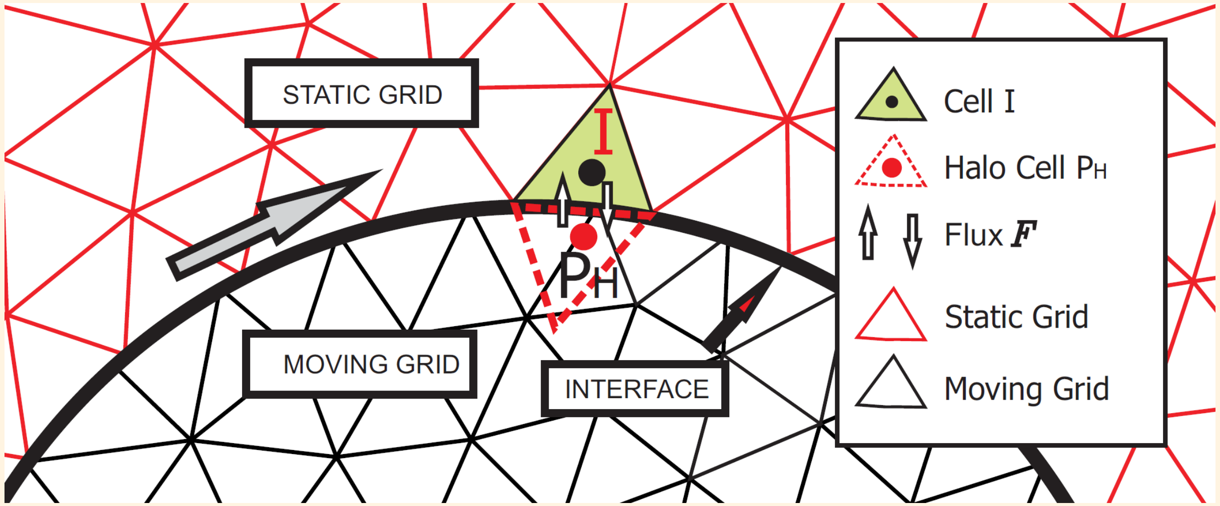

A MLS-based sliding mesh technique

- $\boldsymbol{U}_{P_H}$ is defined as

$$\boldsymbol{U}_{P_H} = \frac{1}{A_{P_H}} \int \boldsymbol{U} dA = \frac{1}{A_{P_H}} \int \sum_{j=1}^{n_x} N_j(\boldsymbol{x}_{P_H}) U_j dA$$

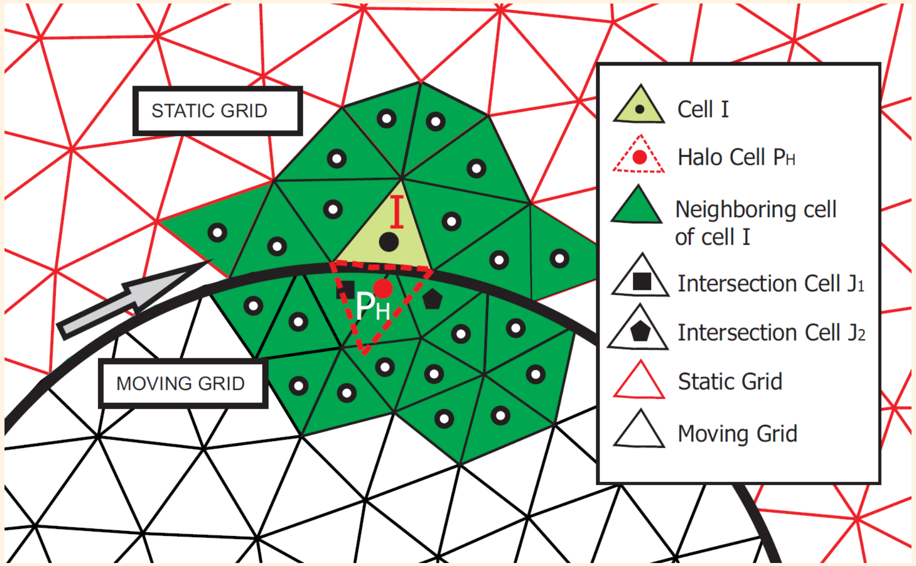

- It avoids the computation of intersection points!

▶ 1D Steady Shock

- Initial Conditions

$$
\begin{aligned}
\rho_L &= 1, & \rho_R &= 1.8621 \\
u_L &= 1.5, & u_R &= 0.8055 \\
p_L &= 0.71429, & p_R &= 1.7559
\end{aligned}
$$

- Computational domain $0 \leq x \leq 10$ discretized in two regions of 25 elements
- The Interface is located at $x = 5.0$

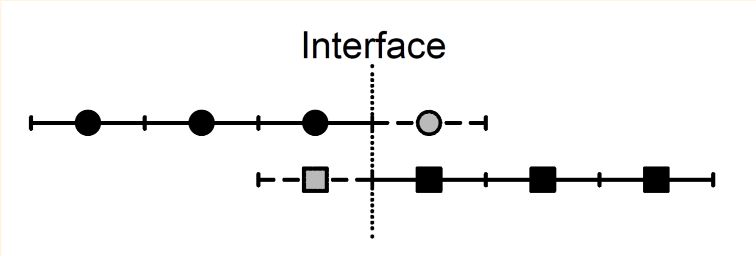

Z.J.Wang et al.. Recent development on the conservation property of chimera. IJCFD, 15,265-278,2001.

Numerical Examples

- 1D Steady Shock

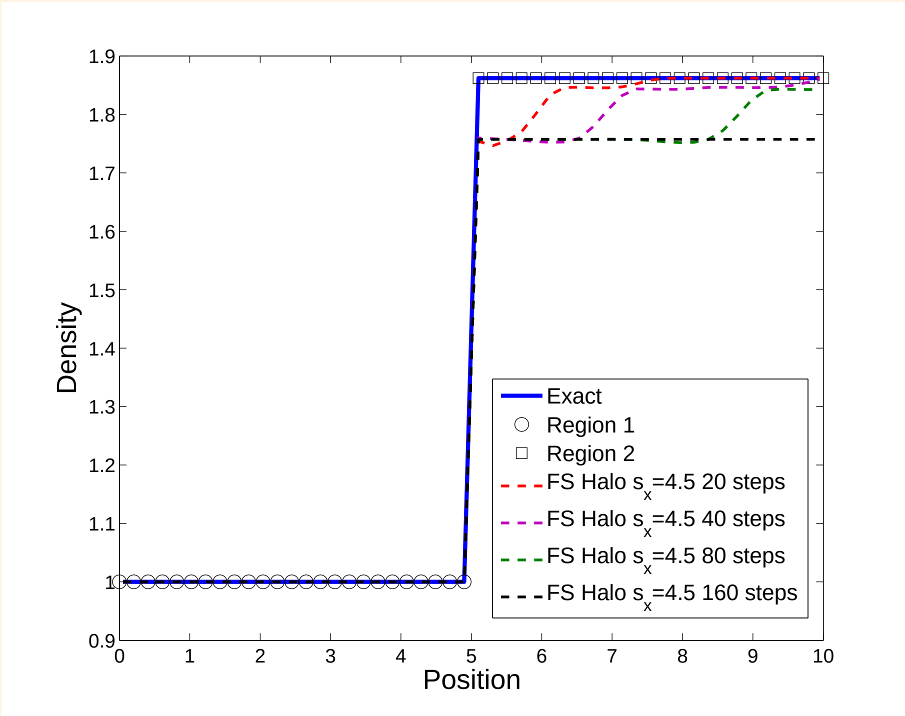

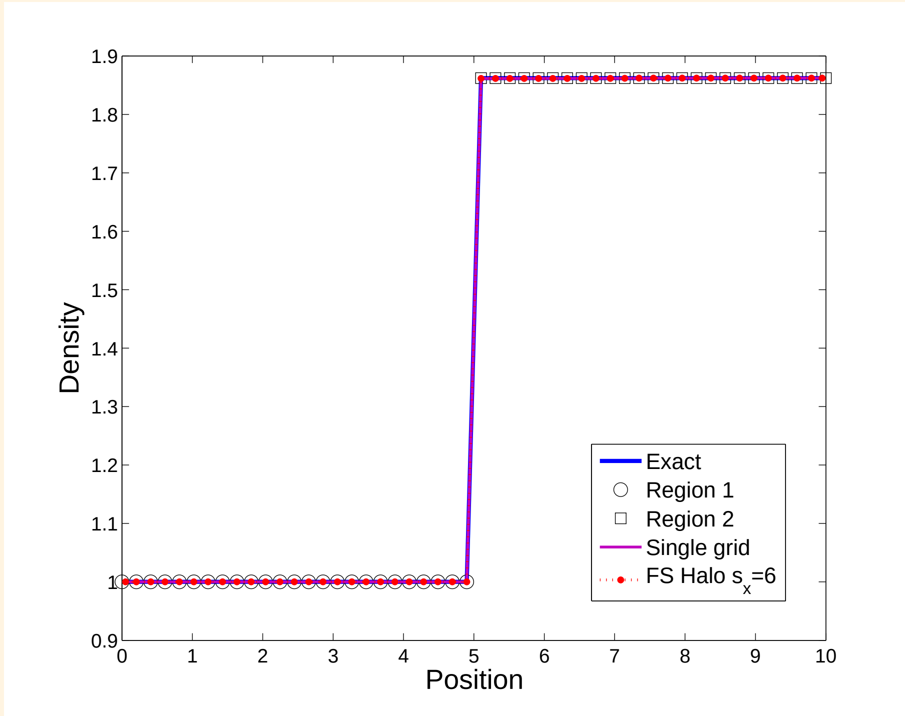

1D Unsteady Shock

- First test case of: *Riemann solvers and numerical methods for fluid dynamics. A practical introduction. Springer,1999.*
- Initial Conditions

$$\begin{array}{rr} \rho_L = 1.0, & \rho_R = 0.125 \\ u_L = 0.75, & u_R = 0.0 \\ p_L = 1.0, & p_R = 0.1 \end{array}$$

- Computational domain $0 \le x \le 1$ discretized in two regions of 150 elements
- The Interface is located at $x = 0.5$

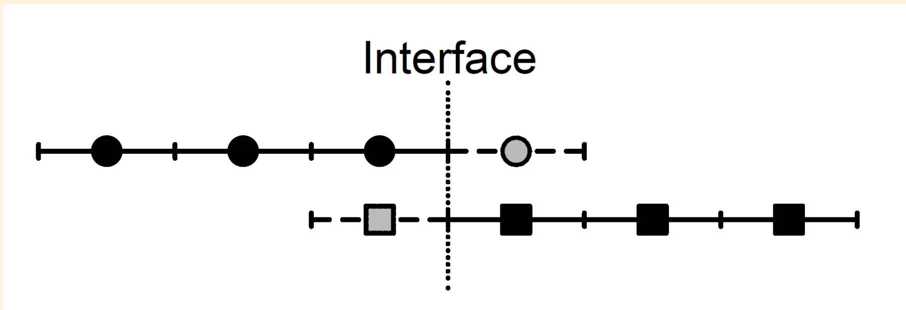

Numerical Examples

- 1D Unsteady Shock

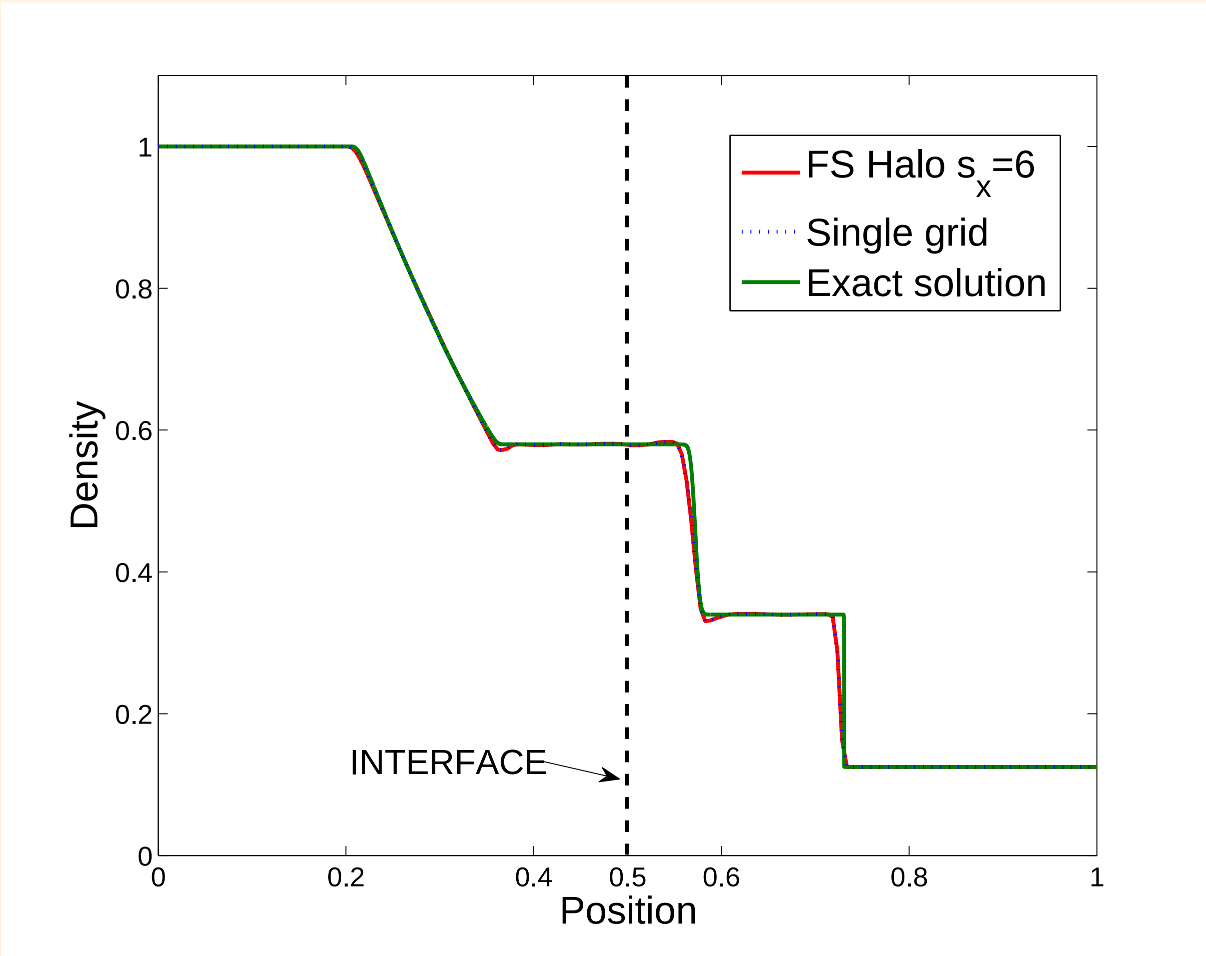

Numerical Examples

- 1D Unsteady Shock

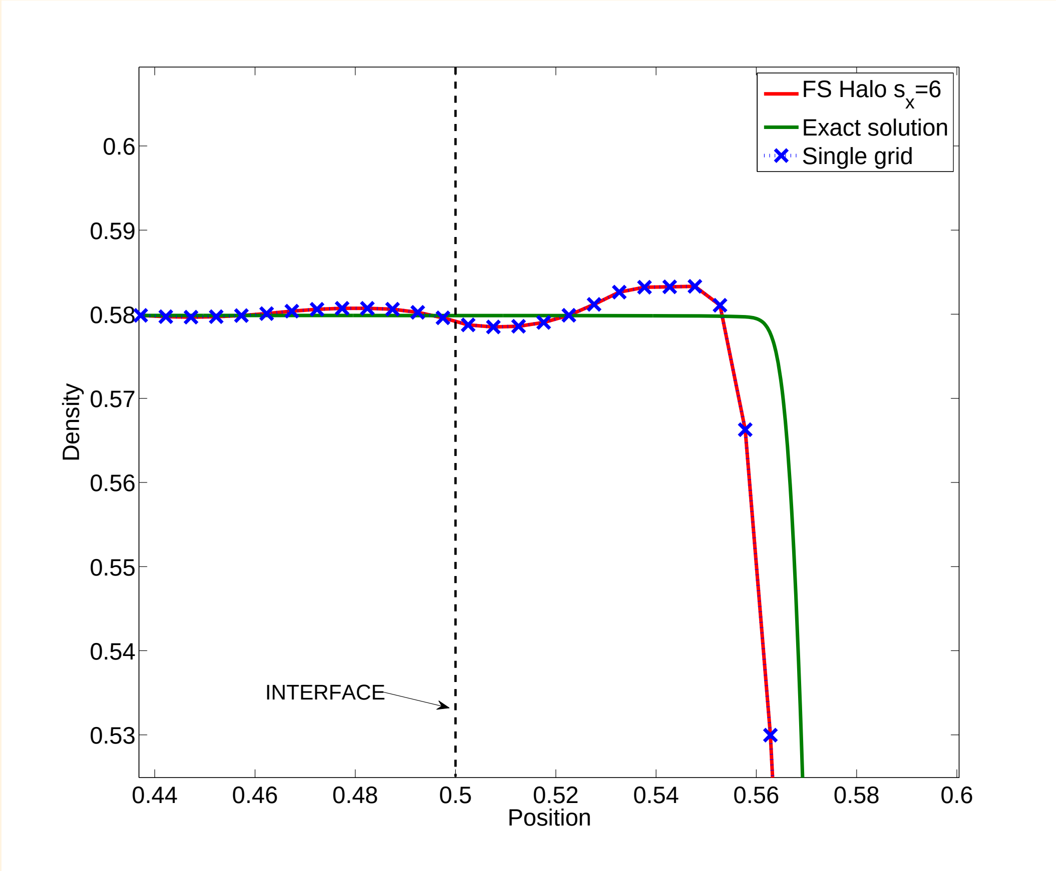

SHARK-FV 2016 Conference
SHARING HIGHER-ORDER ADVANCED RESEARCH KNOW-HOW on FINITE VOLUME
www.math.univ-toulouse.fr/SHARK-FV
Great White
Ofir, Portugal
May 23 - 27, 2016

- Ringleb flow test case

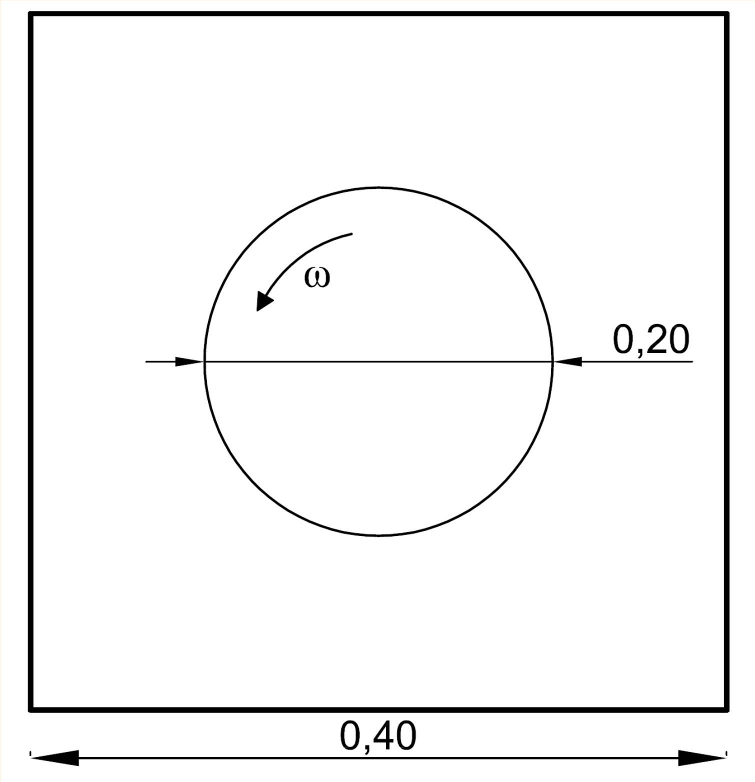

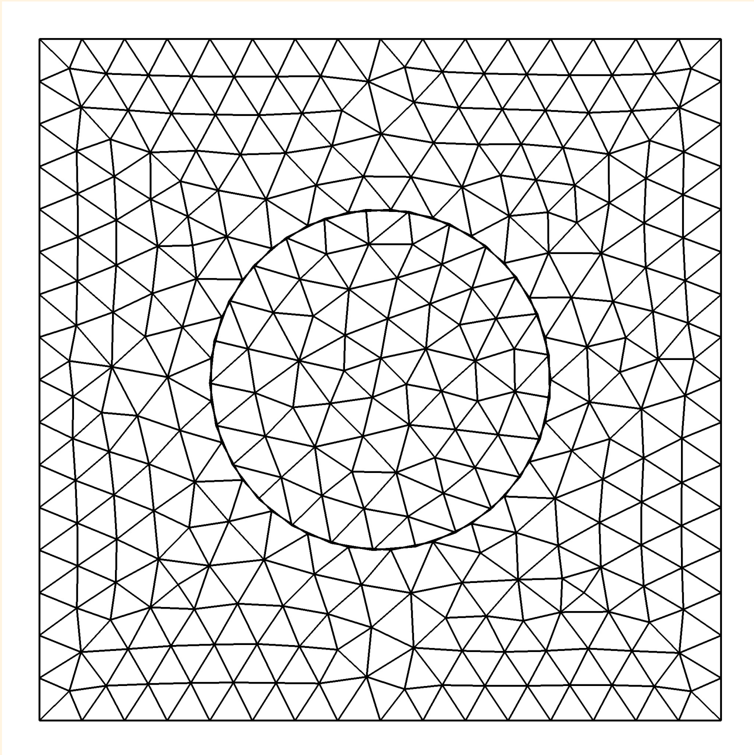

- Ringleb flow test case
  - Third order FV-MLS

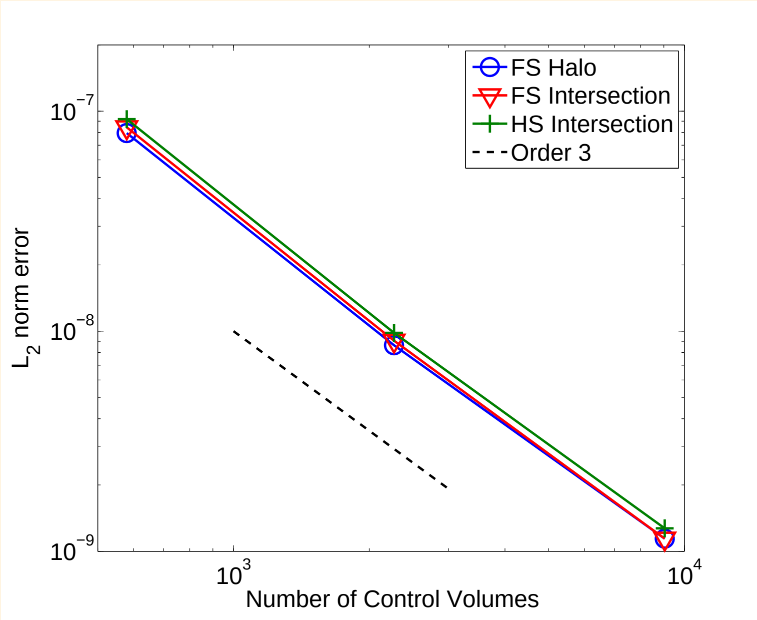

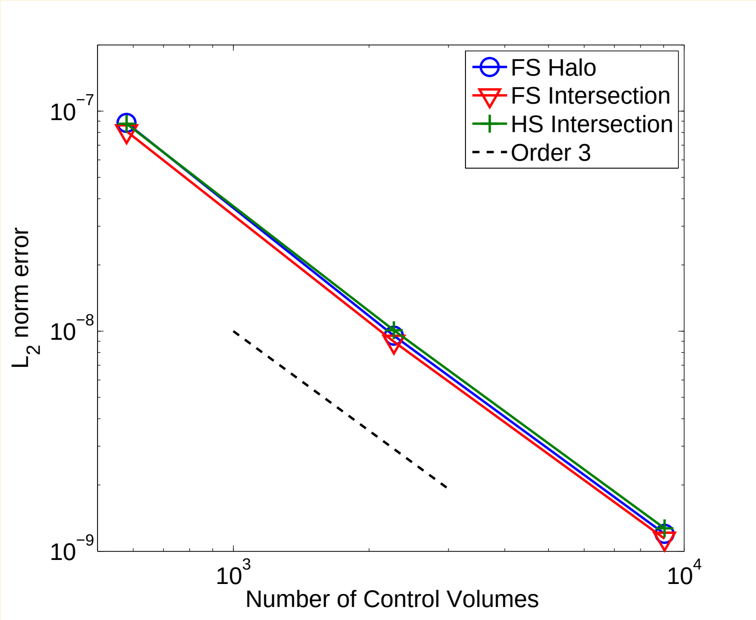

$\omega = 0$ rad/s $\qquad$ $\omega = 0.01$ rad/s

SHARK-FV 2016 Conference
Sharing Higher-order Advanced Research Know-how on Finite Volume
www.math.univ-toulouse.fr/SHARK-FV
Great White
Ofir, Portugal
May 23 - 27, 2016

- Ringleb flow test case
  - Fourth order FV-MLS

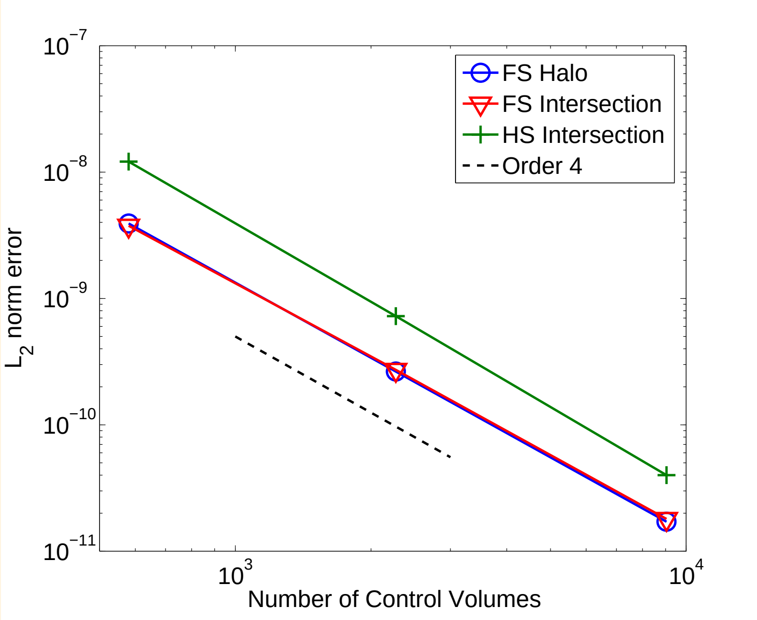

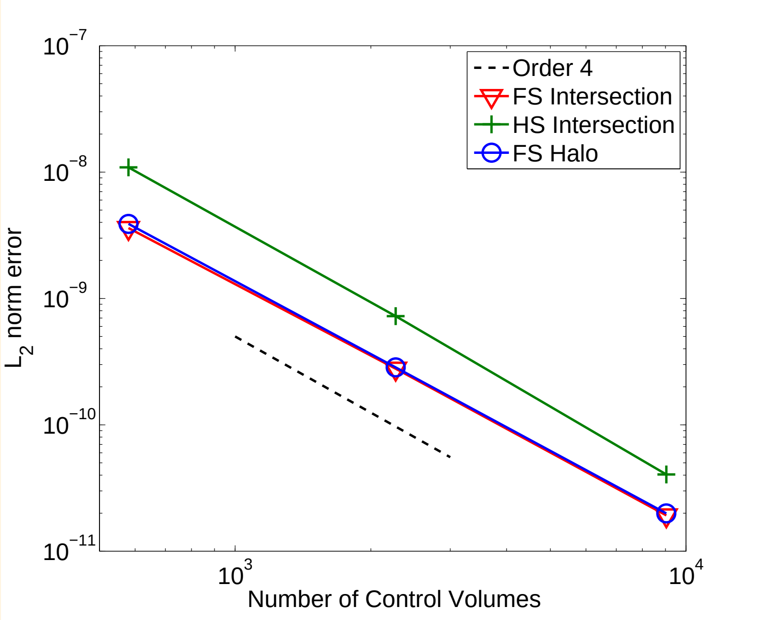

$\omega = 0$ rad/s $\qquad$ $\omega = 0.01$ rad/s

- Ringleb flow test case
  - Conservation Error

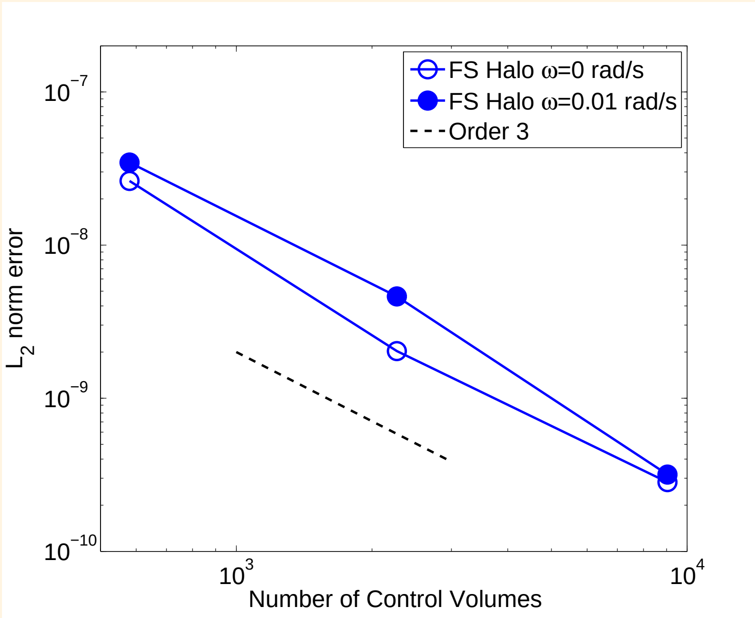

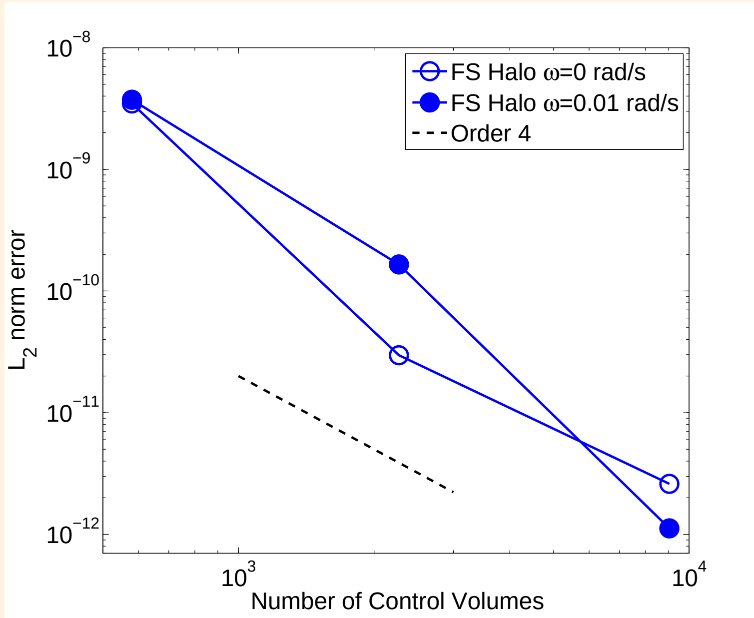

Third order — Fourth order

- 2D Vortex Convection

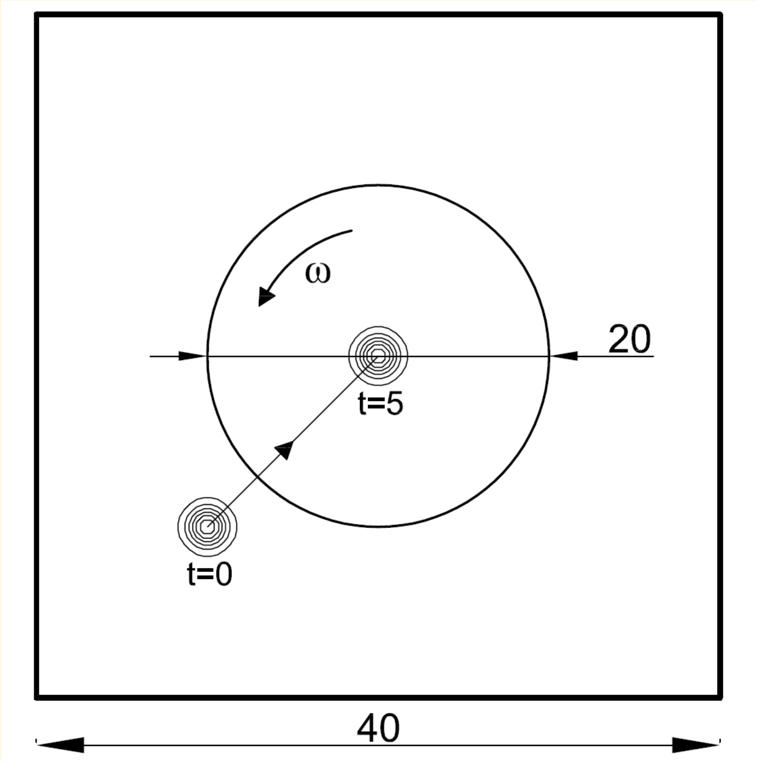

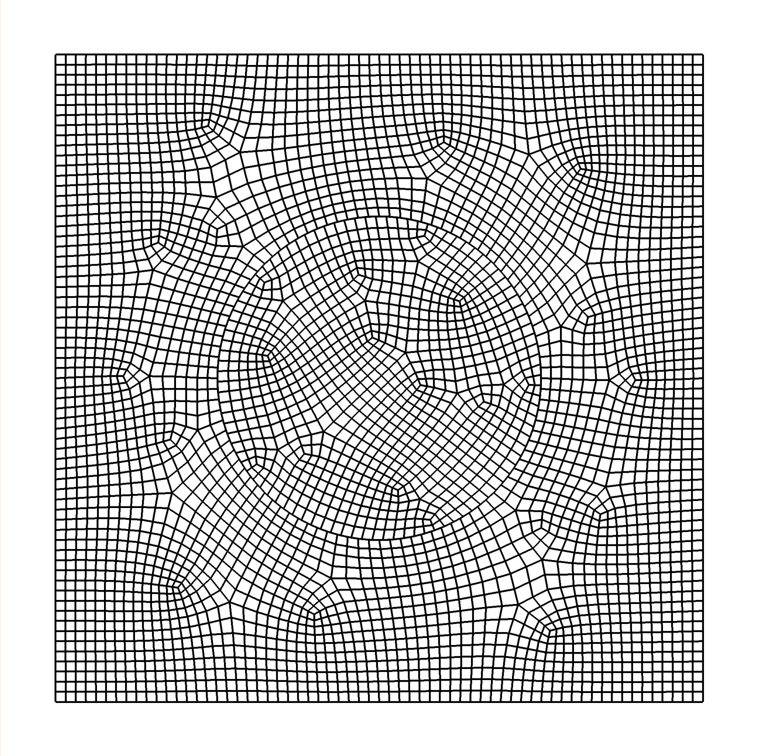

Numerical Examples

- 2D Vortex Convection
  - Third order FV-MLS

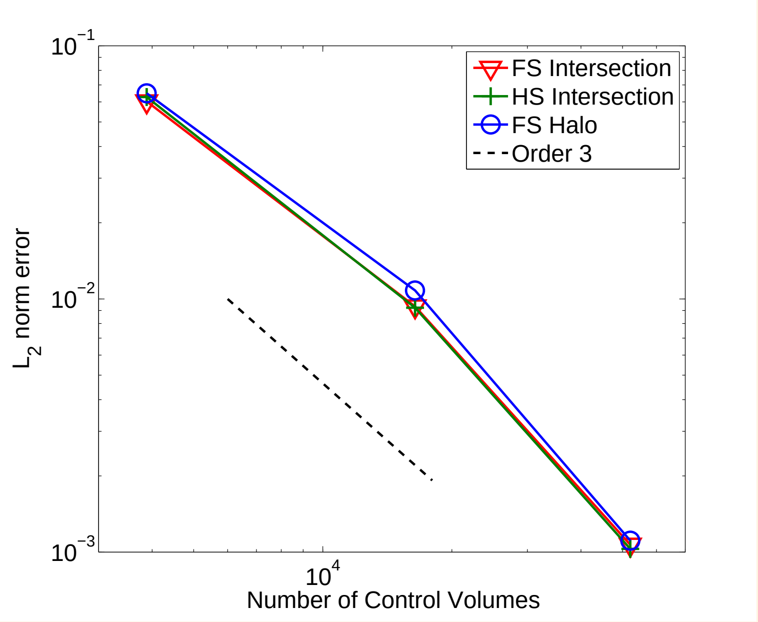

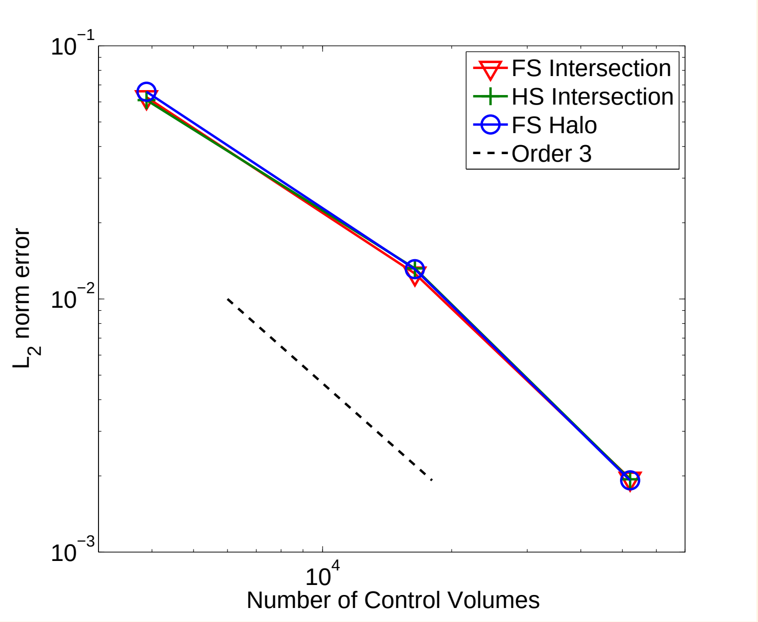

$\omega = 0$ rad/s

$\omega = 1.00$ rad/s

SHARK-FV 2016 Conference
Sharing Higher-order Advanced Research Know-how on Finite Volume
www.math.univ-toulouse.fr/SHARK-FV
Great White
Ofir, Portugal
May 23 - 27, 2016

- 2D Vortex Convection
  - Conservation Error

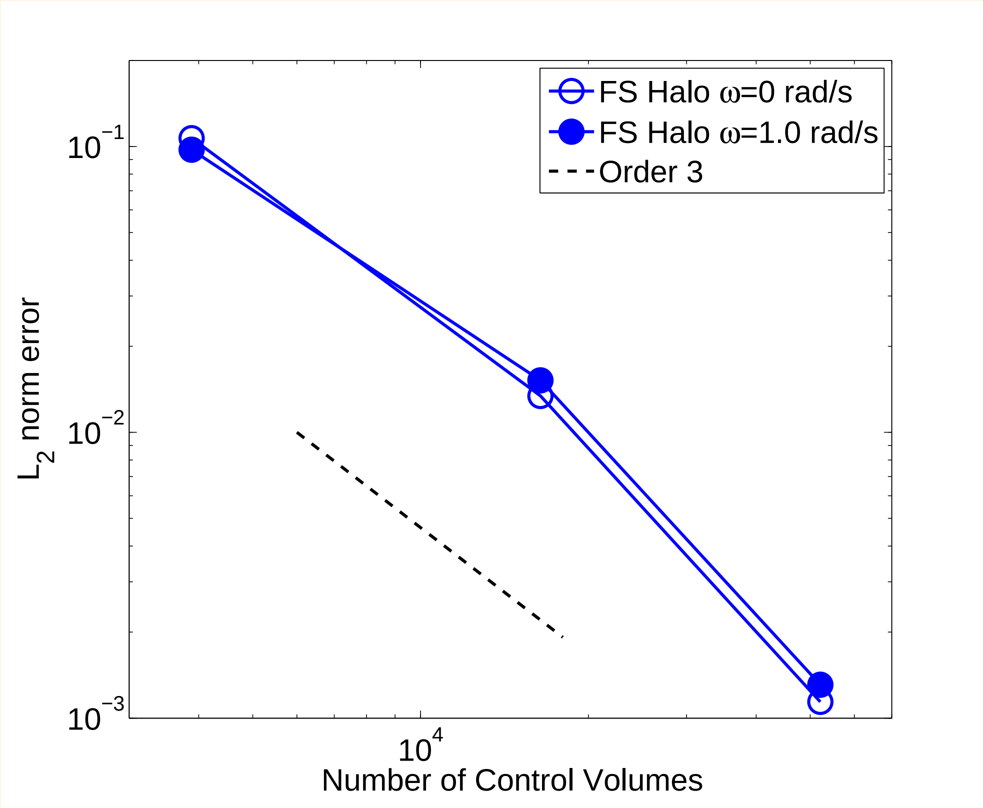

Third order

Numerical Examples

- Supersonic inviscid Flow over a cylinder. Mach 3

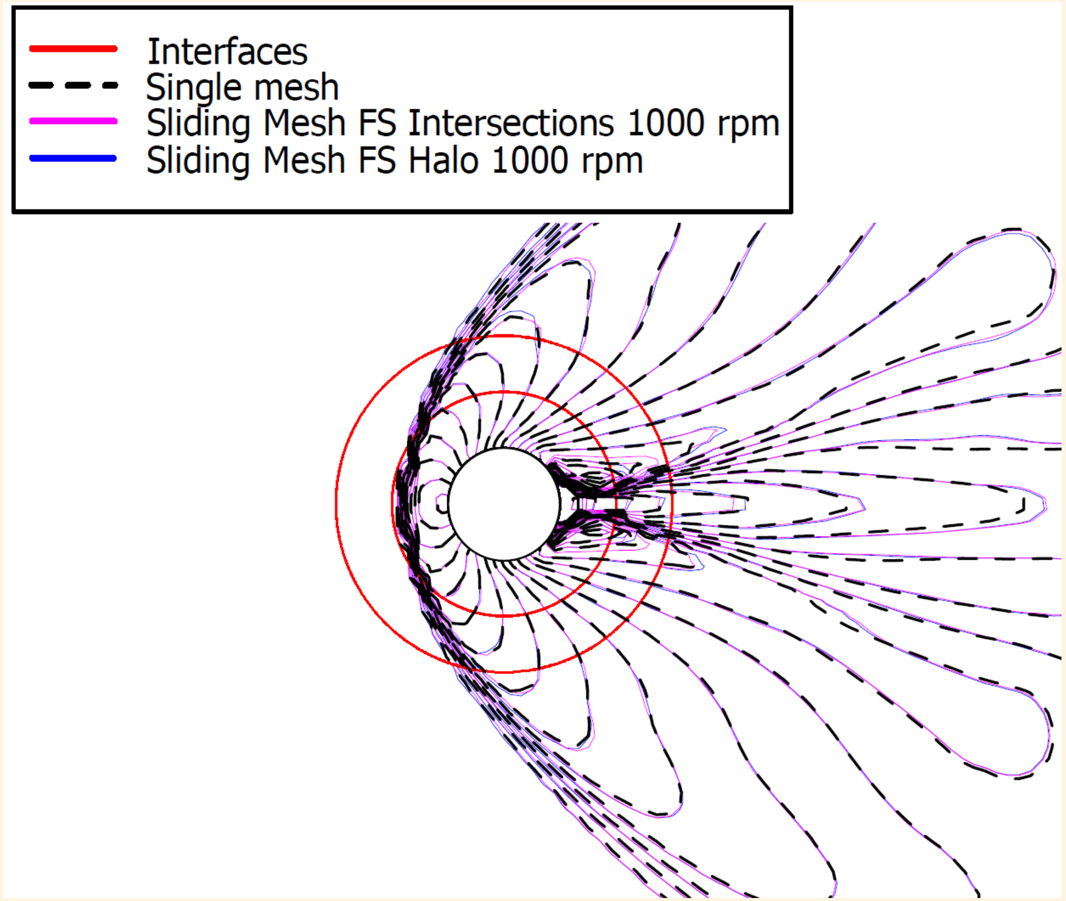

Numerical Examples

- Supersonic Flow over a cylinder. Mach 3

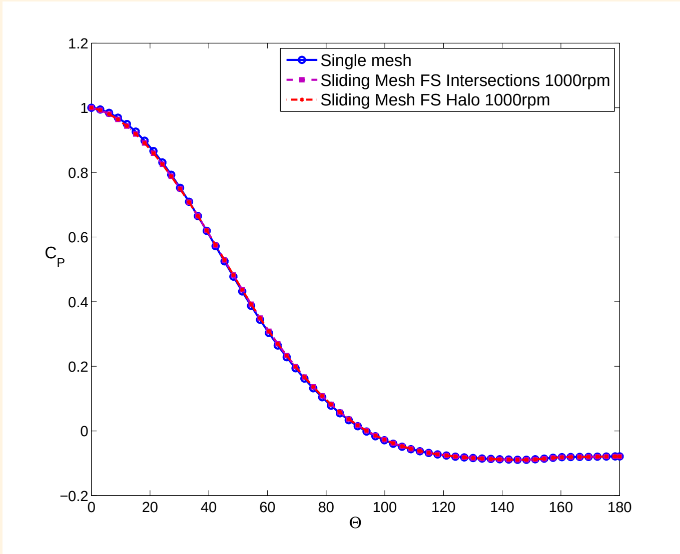

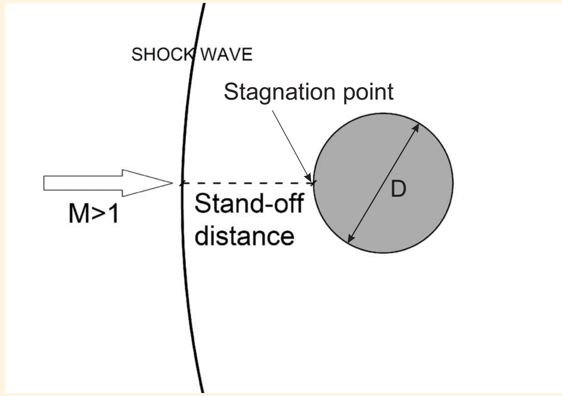

Method	$p_0/(p)_\infty$	Stand-off distance/D
Single mesh	12.015	0.405
Sliding Mesh FS Halo 0 rpm	12.013	0.407
Sliding Mesh FS Halo 1000 rpm	12.013	0.408
Sliding Mesh FS Intersections 1000 rpm	12.013	0.408
Reference solution	12.061	—

- Incompressible flow around a cross-flow turbine.

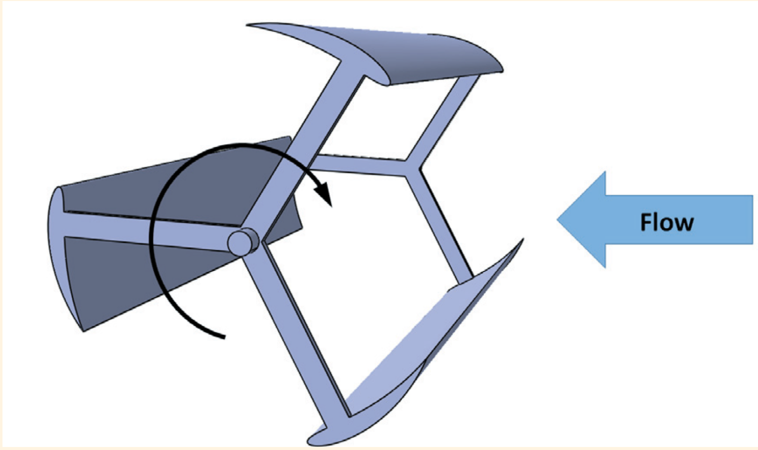

- Two test cases:
  - Single-bladed cross-flow turbine
  - Three-bladed cross-flow turbine

Problems Setup: E. Ferrer et al. A high order discontinuous galerkin fourier incompressible 3D Navier-Stokes solver with rotating sliding meshes. JCP, 231:7037-7056, 2012.

Numerical Examples

- Incompressible flow around a cross-flow turbine.

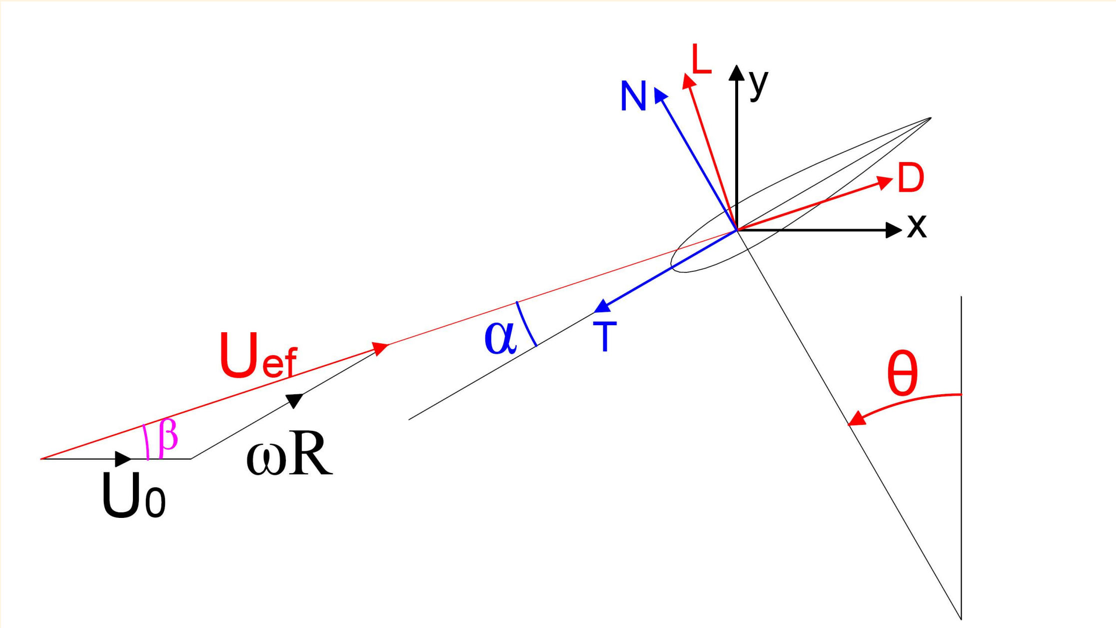

$$\vec{f} = \left\{ \begin{array}{c} f_x \\ f_y \end{array} \right\} = \oint (p\vec{n} - \nu(\nabla\vec{U} \cdot \vec{n}))d\Gamma$$

$$f_N = f_y\cos\theta - f_x\sin\theta \quad f_T = -f_x\cos\theta - f_y\sin\theta$$

- Single-bladed cross-flow turbine
  - Problem setup:

Free-stream velocity U_0	Rotational Speed ω	Tip Speed Ratio $\lambda = \omega R/U_0$
0.2	0.5	5
0.5	0.5	2
1.0	0.5	1

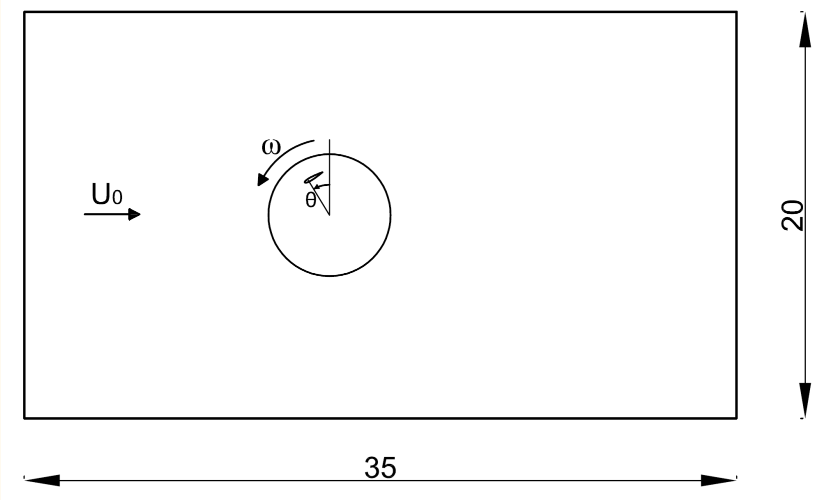

Numerical Examples

- Single-bladed cross-flow turbine

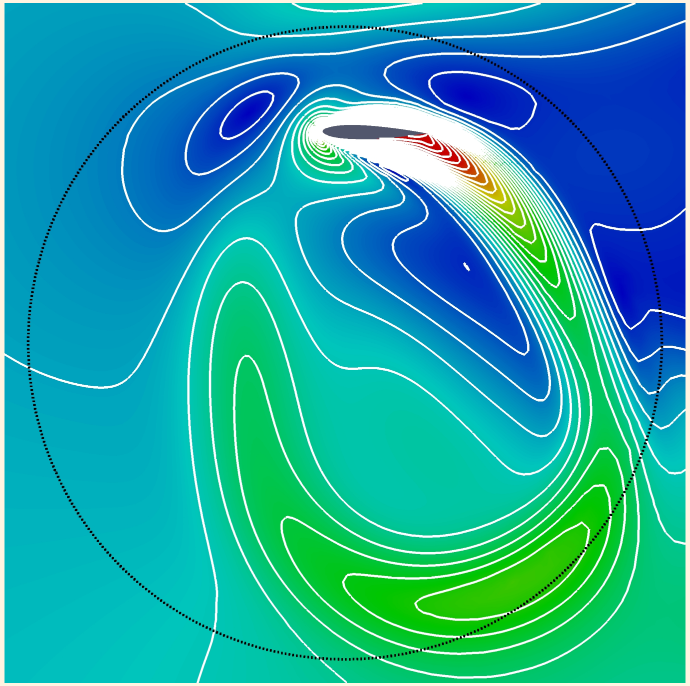

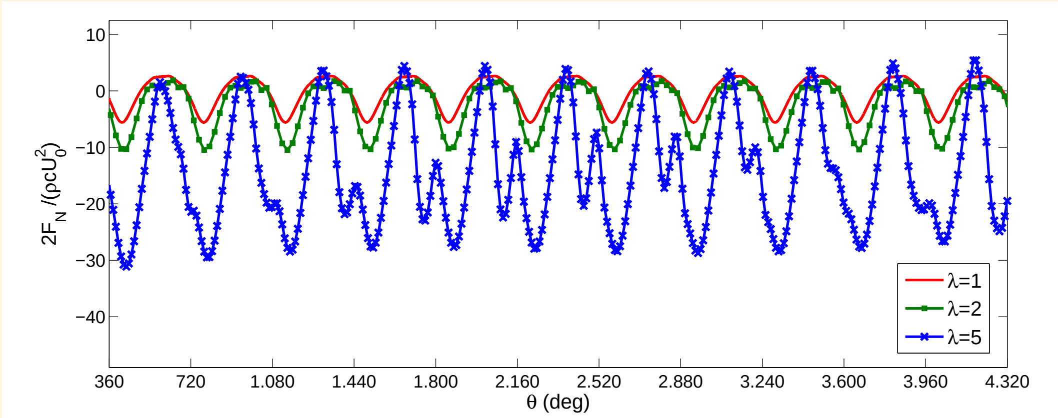

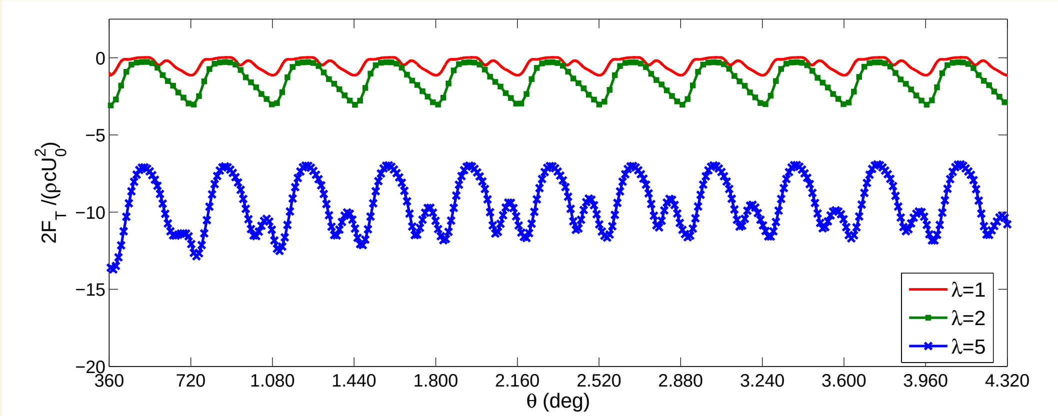

- Three bladed cross-flow turbine
  - Problem setup:
    - $U_0 = 0.5$ m/s
    - $Re = 50$
    - $\omega = 0.5$ rad/s $\rightarrow$ Tip-Speed Ratio (TSR)$= \frac{\omega R}{U_0} = 2$

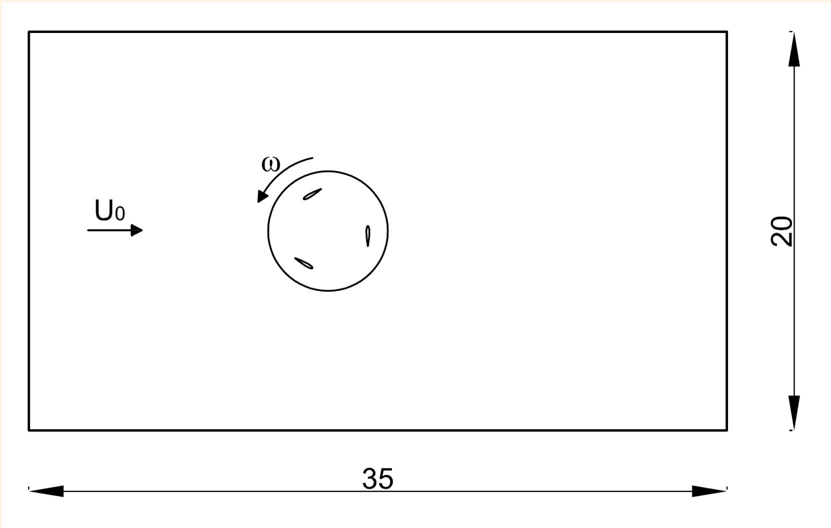

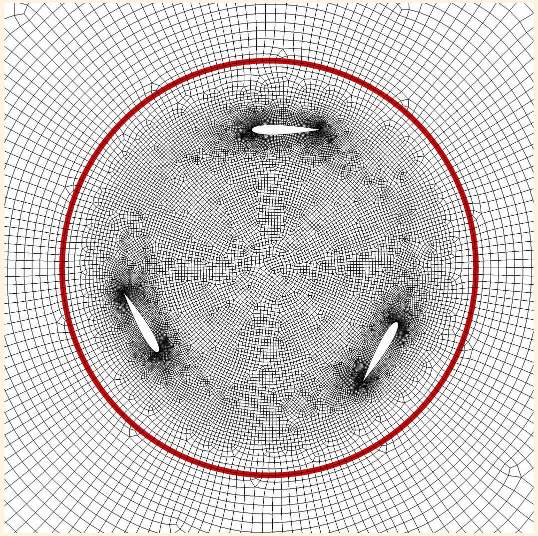

- Three bladed cross-flow turbine

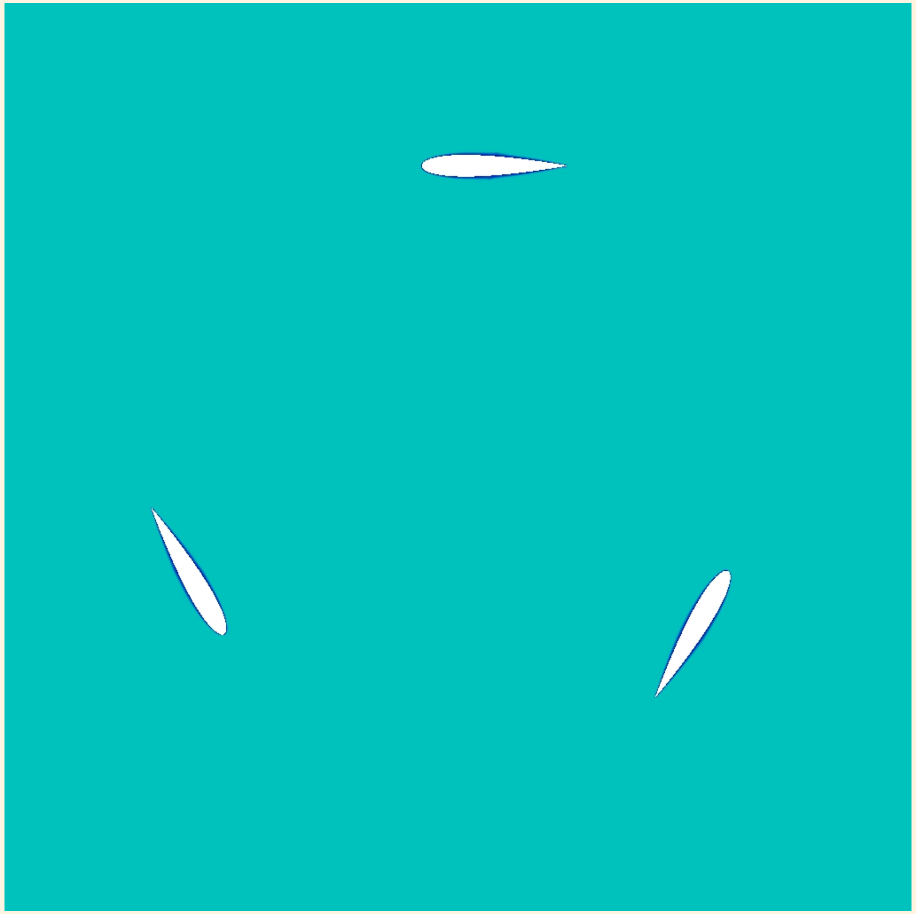

- Fluid-Structure Interaction (FSI)
  - Previous computations $\rightarrow \begin{cases} \omega = \text{given value} \\ \frac{\partial \omega}{\partial t} = 0 \end{cases}$

Fluid-Structure Interaction (FSI)

- Flow driven approach $\rightarrow$ ω given by the fluid

$$\omega^{n+1} = \omega^{n} + \frac{(T - M)\ \Delta t}{J}$$

- T $\rightarrow$ Torque
- M $\rightarrow$ Loading Moment
- Δt $\rightarrow$ Time step
- J $\rightarrow$ Mass moment of inertia

High-order Fluid-Structure-Interaction techniques

- Fluid-Structure Interaction (FSI)

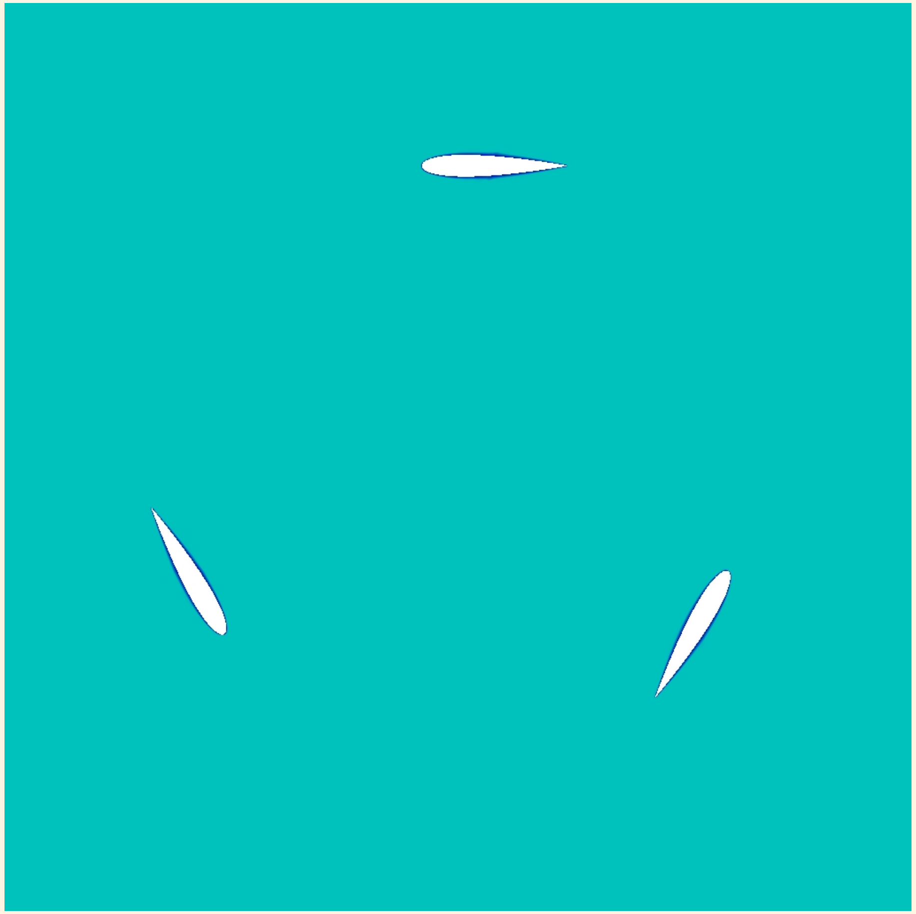

High-order Sliding Mesh techniques

- The MLS-based intersection sliding mesh technique:
  - ▷ The Half-Stencil avoids the recomputation of stencils and MLS approximations
  - ▷ The Half-Stencil is less accurate
- The Interface halo cell sliding mesh technique:
  - ▷ Avoids the computation of intersection.
  - ▷ Non-conservative method (Theoretically)
  - ▷ In practice: Conservation error $<$ Variables error
- The capabilities of the new formulation are tested on a cross-flow turbine
- Drawnback: Only useful for simple movements (rotating domains and sliding planes).

- Introduction
- The FV-MLS method
- A MLS-based sliding mesh technique
- A High-order Chimera method
- An immersed boundary method for unstructured meshes
- Conclusions

A High-order Chimera method

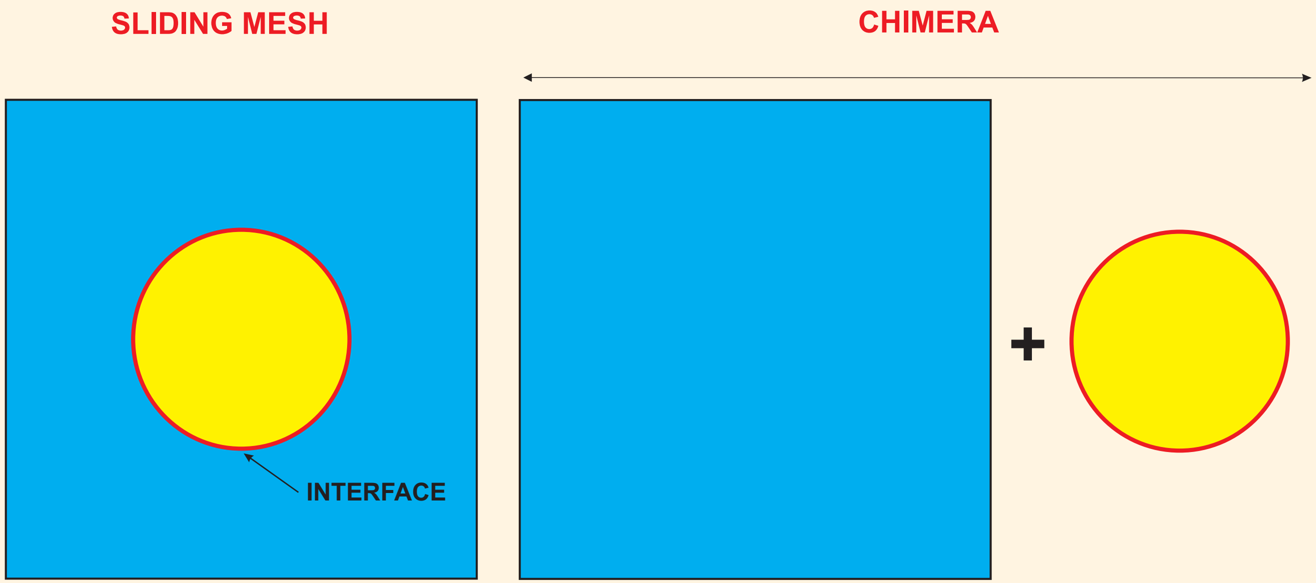

- Chimera methods allows:
  - ▷ Complex movements.
  - ▷ Grid adaptation.
  - ▷ Flexibility.

A High-order Chimera method

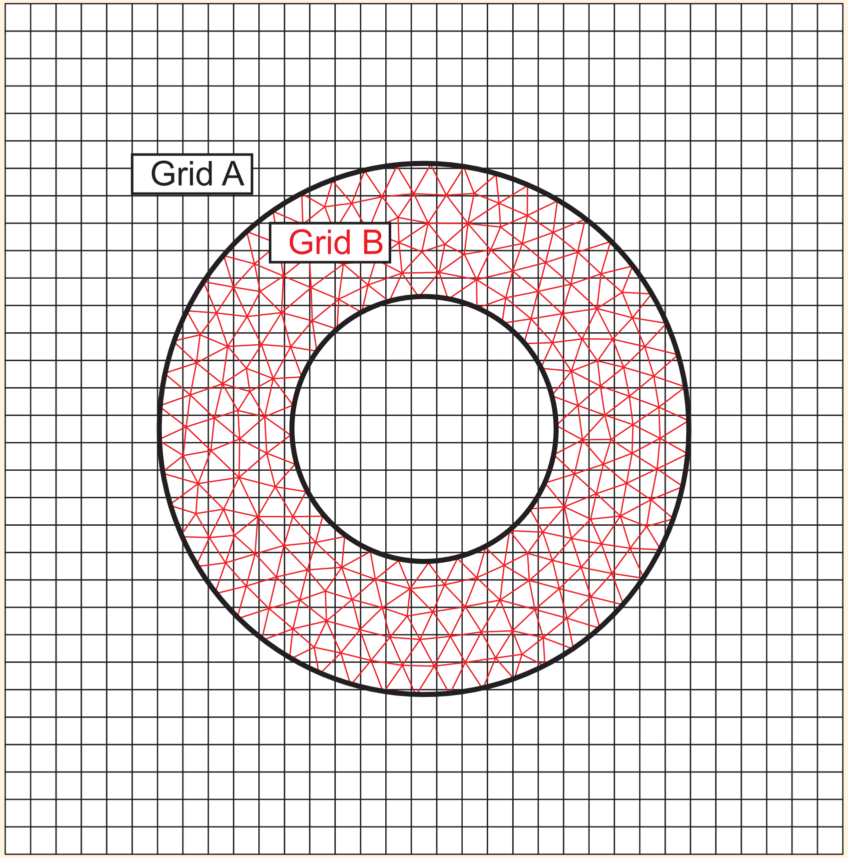

A High-order Chimera method

- Identification of the resolved cells.

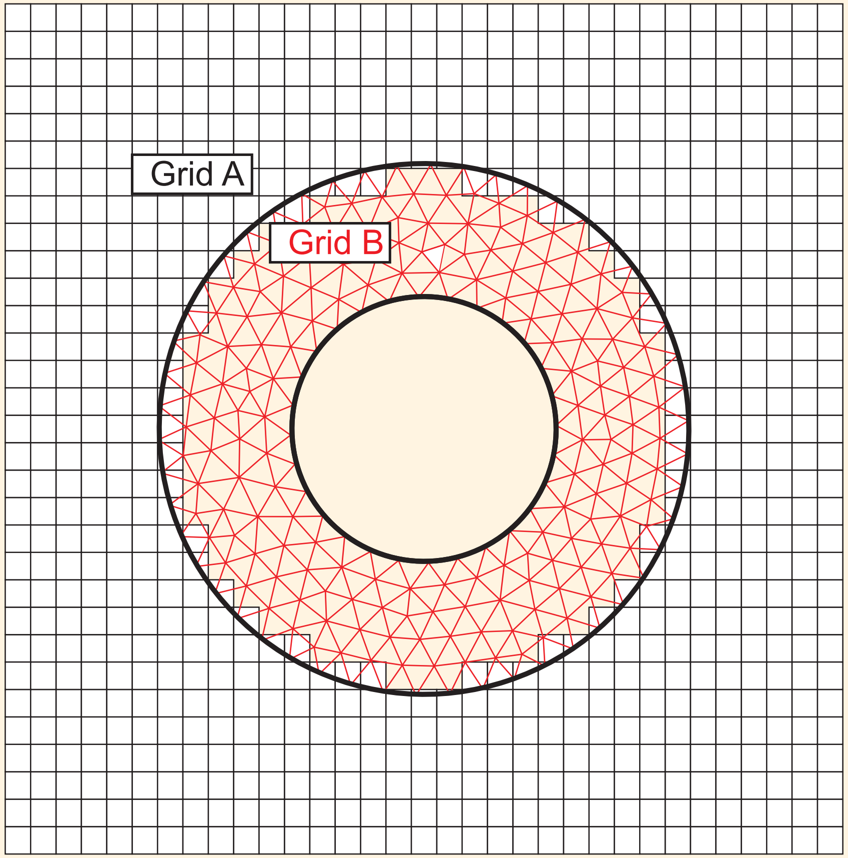

SHARK-FV 2016 Conference
Sharing Higher-order Advanced Research Know-how on Finite Volume
www.math.univ-toulouse.fr/SHARK-FV
Great White
Ofir, Portugal
May 23 - 27, 2016

A High-order Chimera method

- Resolution of the system of conservation laws on each grid.

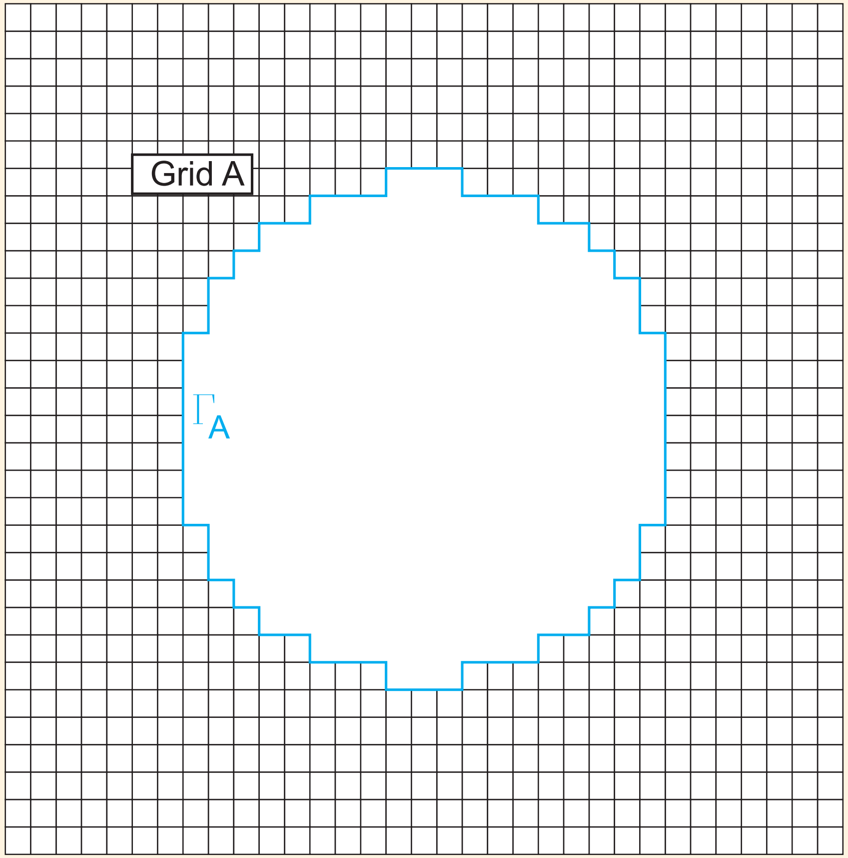

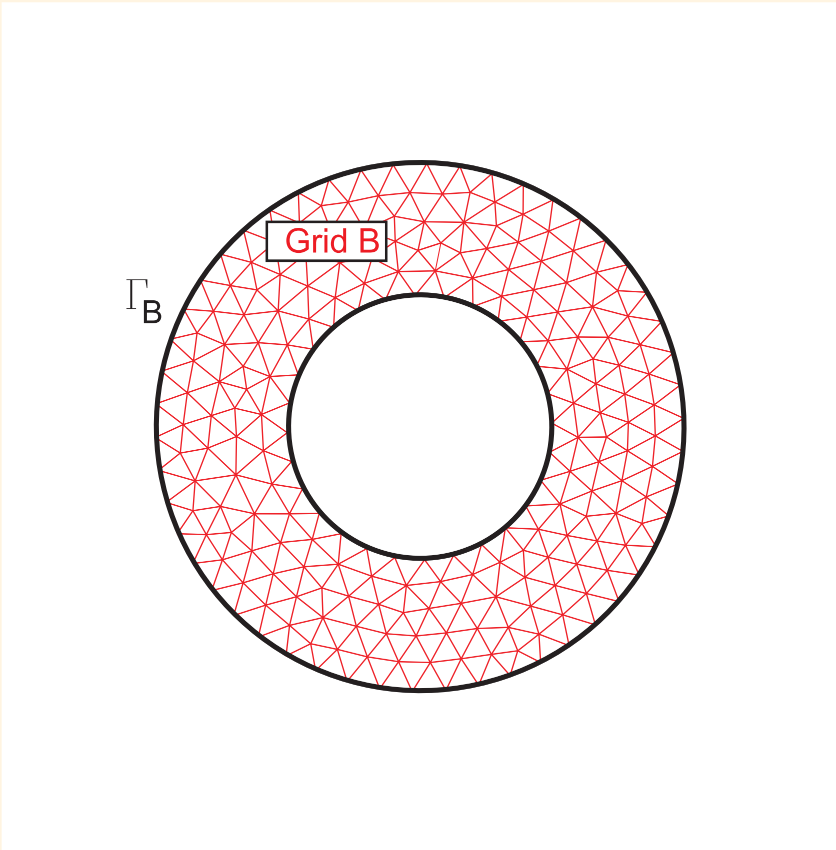

- There is a need to define the fluxes through Γ_A and Γ_B.

A High-order Chimera method

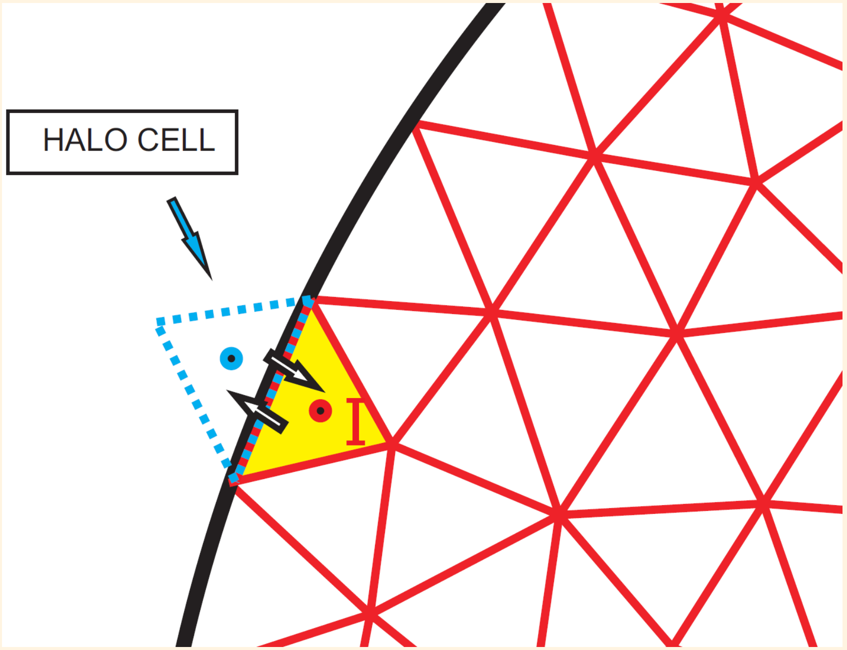

- We use the Halo Cell approach.

$$\boldsymbol{U}_{Halo} = \frac{1}{A_{Halo}} \int \boldsymbol{U} dA = \frac{1}{A_{Halo}} \int \sum_{j=1}^{n_x} N_j(\boldsymbol{x}_{Halo}) U_j dA$$

- Once the equations are solved the solution is approximated using on each unresolved cell.

Numerical Examples

▶ 2D Isentropic Vortex Convection.

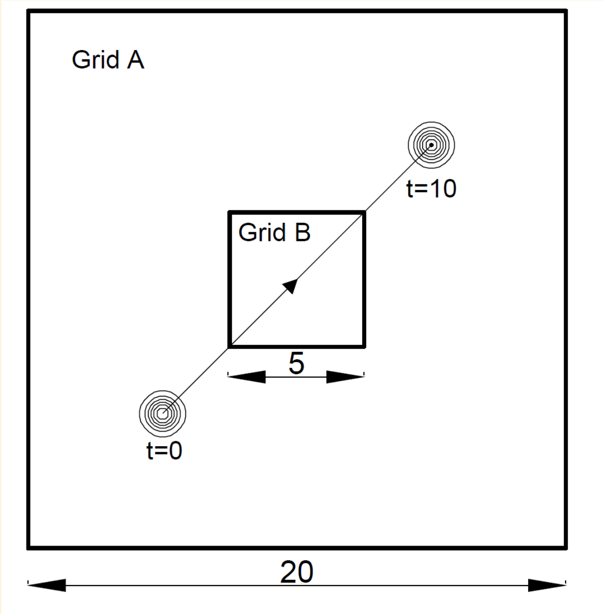

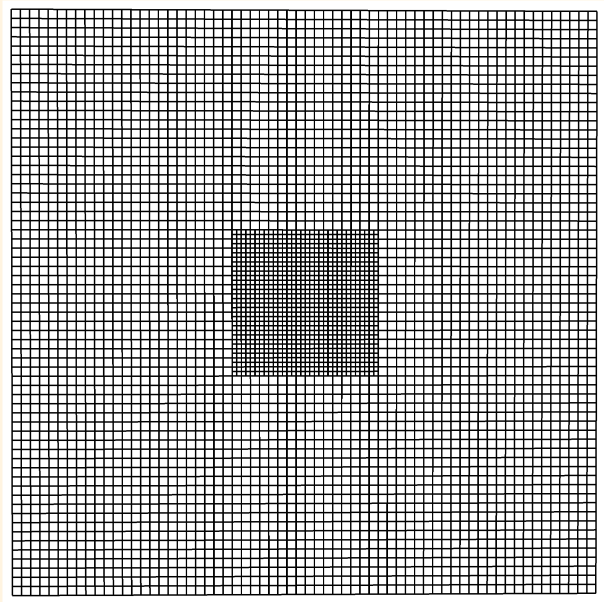

- Two test cases:
  - ▷ No Motion
  - ▷ Prescribed Motion Grid B→ $(x, y) = (0, A\sin(2\pi f t))$, $A = 1$ $f = 0.5$

- 2D Isentropic Vortex Convection.

Isentropic Vortex Convection		
Mesh	$GridA$ $(N_x \times N_y)_A$	Grid B $(N_x \times N_y)_B$
Mesh 1	64×64	32×32
Mesh 2	96×96	48×48
Mesh 3	128×128	64×64

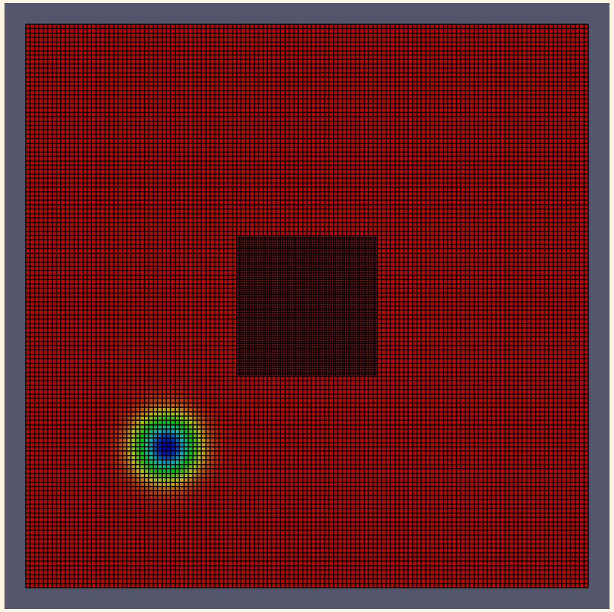

- 2D Isentropic Vortex Convection.3^{rd} order FV-MLS

No motion		
Solved Cells	$L_2 Error$	Order
4864	1.89×10^{-2}	$--$
10944	5.07×10^{-3}	3.25
19456	1.77×10^{-3}	3.67

Prescribed motion		
Solved Cells	$L_2 Error$	Order
4910	1.87×10^{-2}	$--$
11014	5.39×10^{-3}	3.08
19550	2.00×10^{-3}	3.46

SHARK-FV 2016 Conference
Sharing Higher-order Advanced Research Know-how on Finite Volume
www.math.univ-toulouse.fr/SHARK-FV
Great White
Ofir, Portugal
May 23 - 27, 2016

- 2D Isentropic Vortex Convection. 3^{rd} order FV-MLS

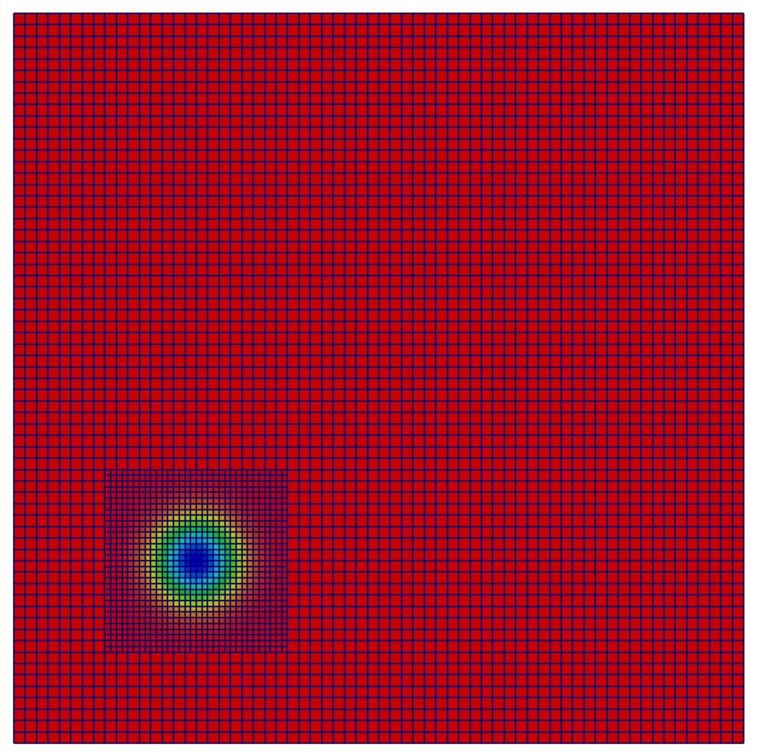

Prescribed motion		
Solved Cells	$L_2 Error$	Order
4895	3.28×10^{-3}	$--$
11036	9.45×10^{-4}	3.06

▶ Subsonic Inviscid flow around NACA 0012

- $M_\infty = 0.63$
- $\alpha = 2°$
- O-mesh $R = 30c$
- Single Mesh: 16601 cells.
- Chimera:15444 solved cells.

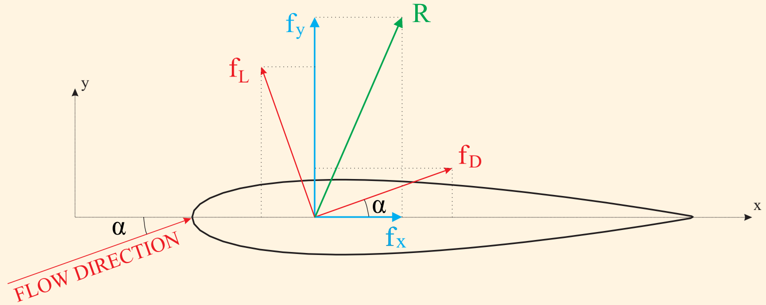

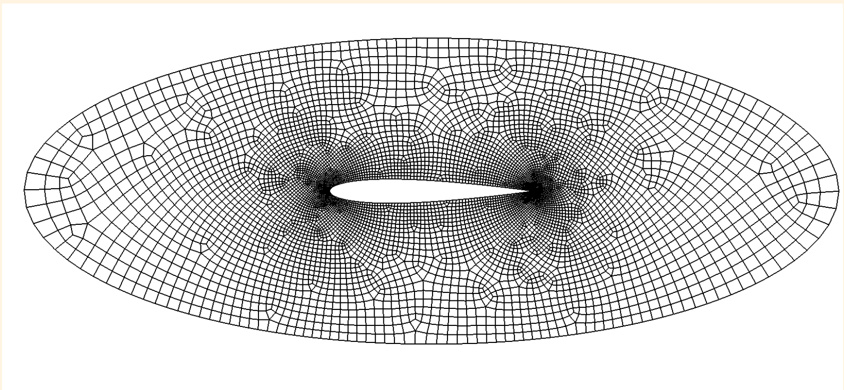

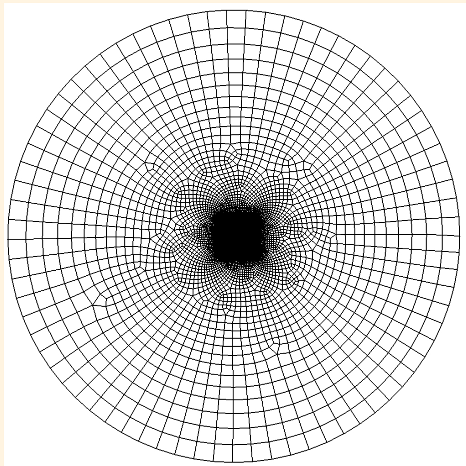

Numerical Examples

- Subsonic Inviscid flow around NACA 0012

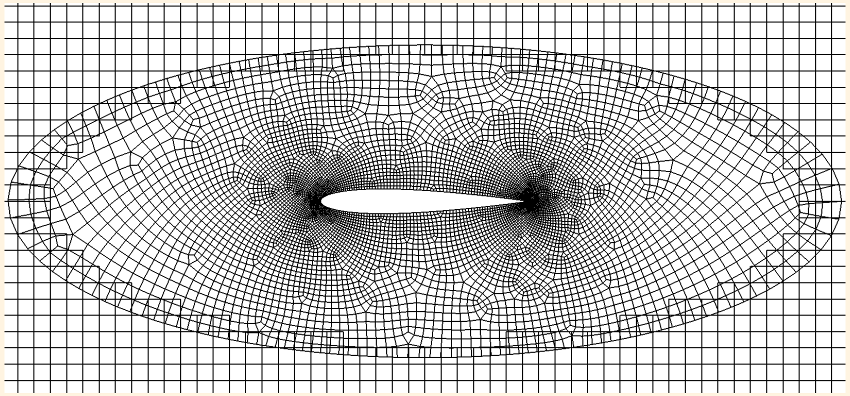

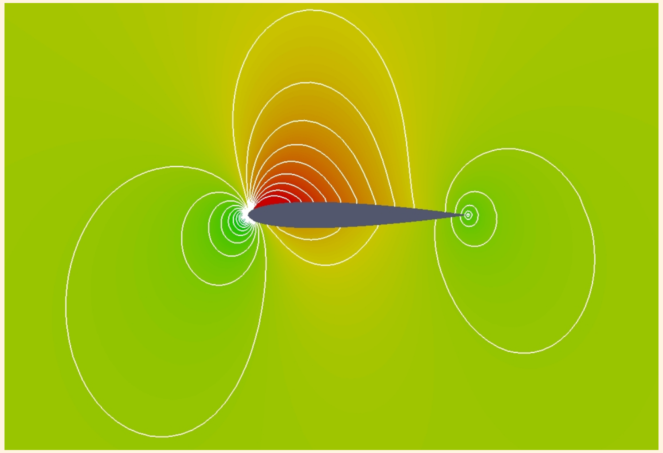

Method	C_L	C_D
Single mesh	0.3248	2.2835×10^{-4}
Chimera	0.3248	2.3069×10^{-4}
Reference solution	0.335	0.0

Numerical Examples

- Supersonic Flow over a cylinder. Mach 3

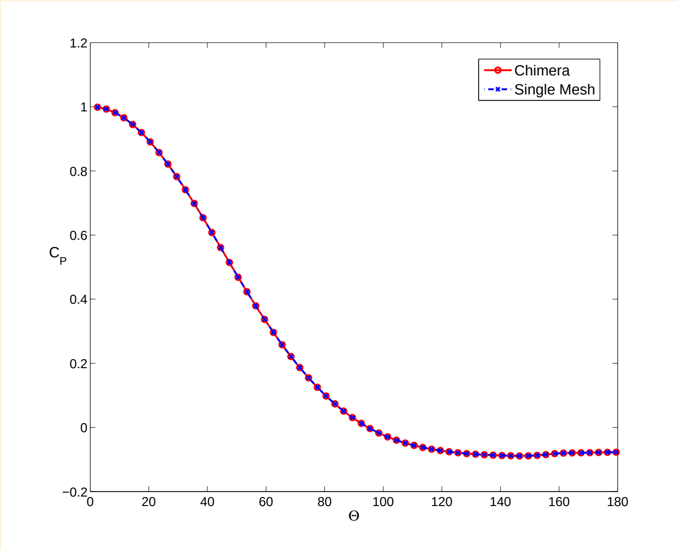

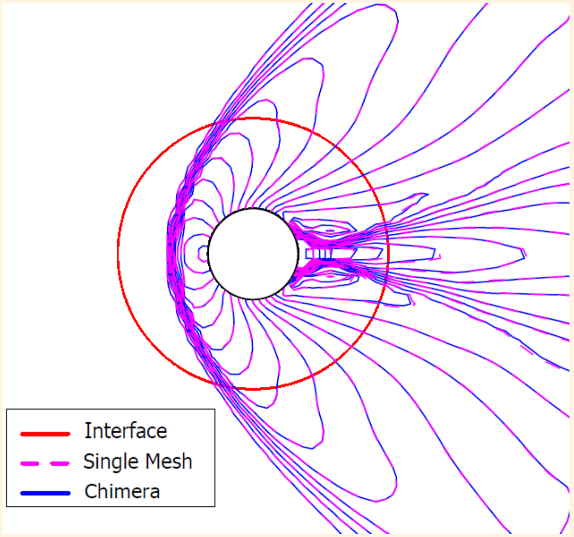

Method	$p_0/(p)_\infty$	Stand-off distance/D
Single mesh	11.888	0.415
Chimera Mesh	11.886	0.416
Reference solution	12.061	—

- Steady Laminar flow around a cylinder.
  - $M_\infty = 0.1$
  - $Re = 40$

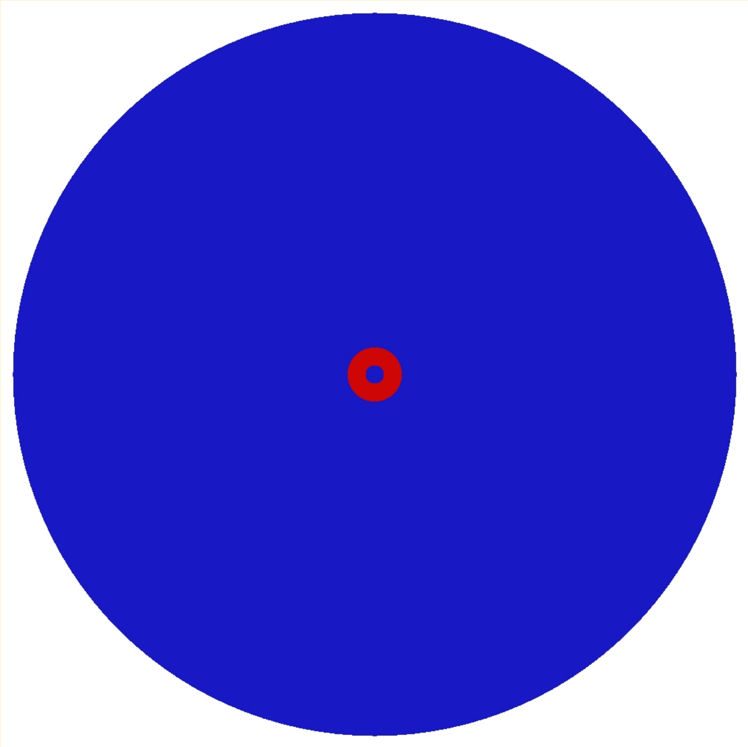

13774 cells

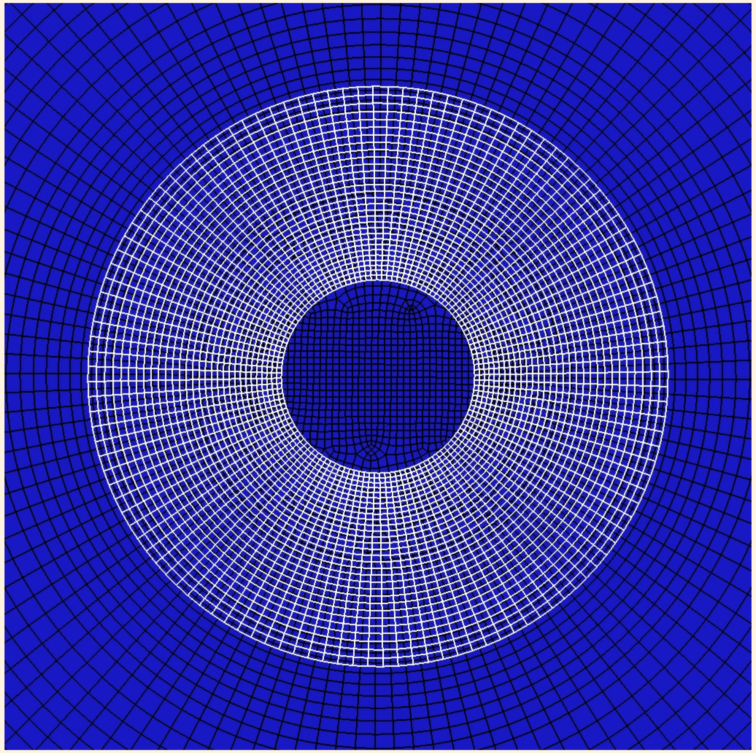

3600 cells

Numerical Examples

- Steady Laminar flow around a cylinder.

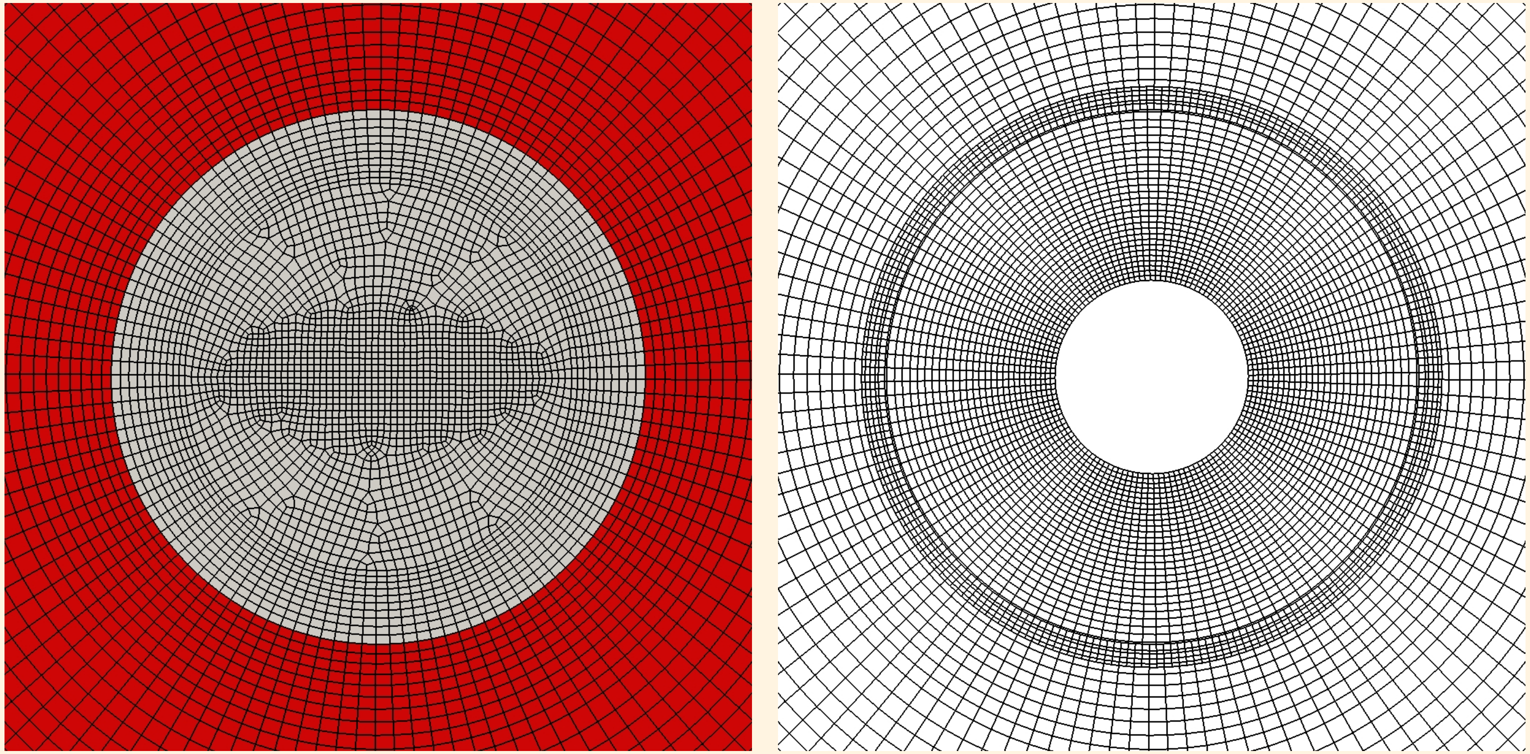

Numerical Examples

- Steady Laminar flow around a cylinder.

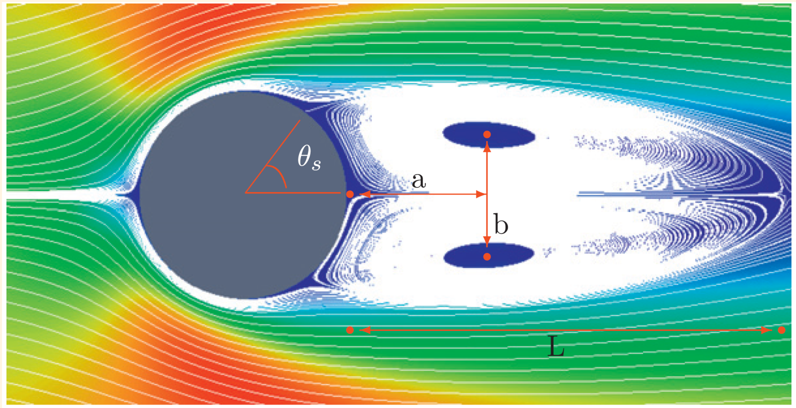

Method	C_D	L/R	$2b/D$	$2a/D$	θ_s	$C_p(0)$	$C_p(\pi)$
Chimera	1.568	4.20	1.168	1.264	52.69 deg	−0.512	1.180
Reference [1]	1.574	–	–	–	–	−0.555	1.147
Reference [2]	1.499	4.49	–	–	52.89 deg	−0.487	1.133
Reference [3]	1.565	4.3	1.17	1.34	52.71 deg	−0.516	1.205

An immersed boundary method for unstructured meshes

- Introduction
- The FV-MLS method
- A MLS-based sliding mesh technique
- A High-order Chimera method
- An immersed boundary method for unstructured meshes
- Conclusions

An immersed boundary method for unstructured meshes

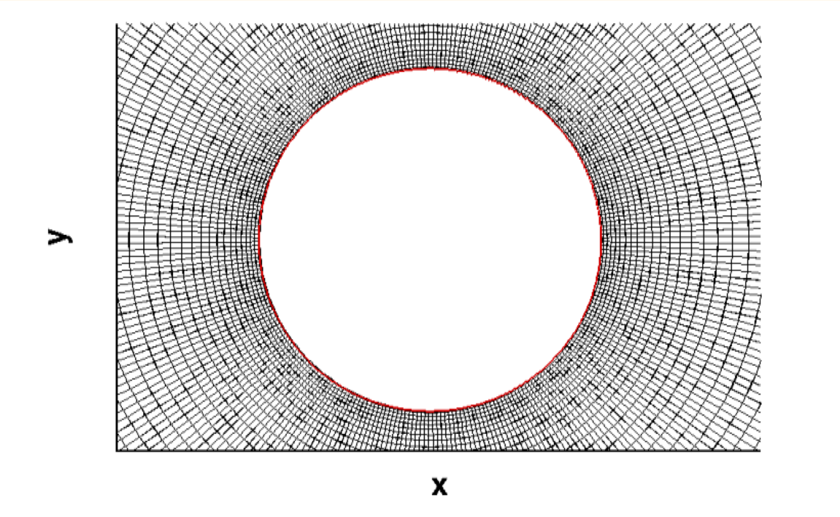

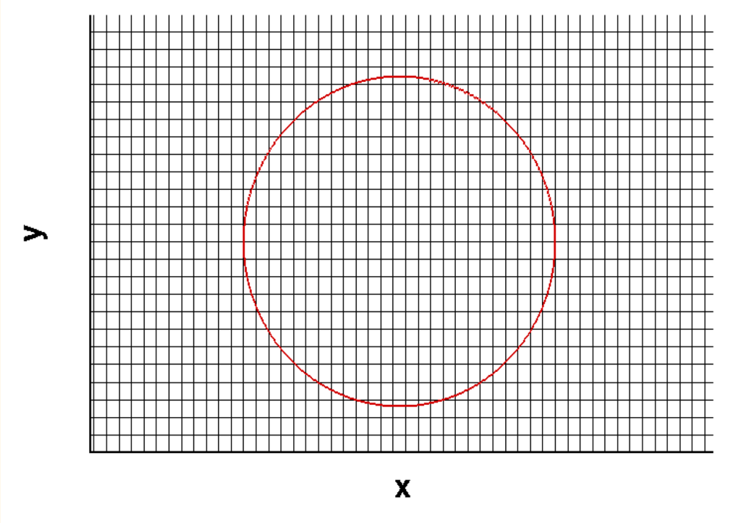

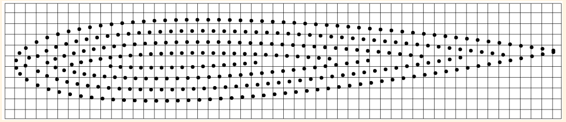

- Immersed boundaries:
  - Complex movements.
  - Grid adaptation.
  - Flexibility.
  - Less accurate:
    - No body-fitted meshes.
    - Highly dependent of interpolation functions.

- Multi-step predictor-corrector procedure:
  - ▷ Computation of the predicted Eulerian velocities ($\tilde{\boldsymbol{u}}$) from the momentum equations.

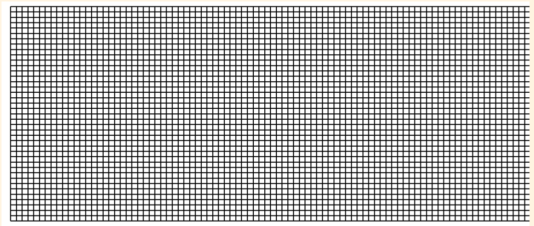

- Interpolate the predicted velocities ($\tilde{\boldsymbol{u}}$) to the Lagrangian points using:
  - ▷ Delta-functions
  - ▷ MLS

$$\tilde{\boldsymbol{u}}_L = \sum_{j=1}^{n_e} \mathbf{N}_j^T(\mathbf{x}_j - \mathbf{X}_L)\tilde{\boldsymbol{u}}_j$$

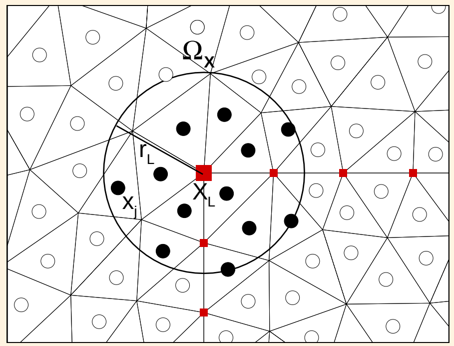

An immersed boundary method for unstructured meshes

- Compute the force that the Lagrangian marker L need to exert on the fluid in order to satisfy the B.C. ($\boldsymbol{u}_L$)

$$\tilde{\boldsymbol{F}}_L = \frac{\tilde{\boldsymbol{u}}_L - \boldsymbol{u}_L}{\Delta t} A_L$$

- Transfer the force from the Lagrangian markers to Eulerian cells.

$$\mathbf{f}_j = \sum_{L=1}^{n_L} \mathbf{N}_j^T(\mathbf{x}_j - \mathbf{X}_L)\mathbf{F}_L / a_j$$

- Correct the initial prediction of the Eulerian velocities

$$\boldsymbol{u}_j = \tilde{\boldsymbol{u}}_j + \boldsymbol{f}_j \Delta t.$$

- Application to the shallow water equations. Damm break.

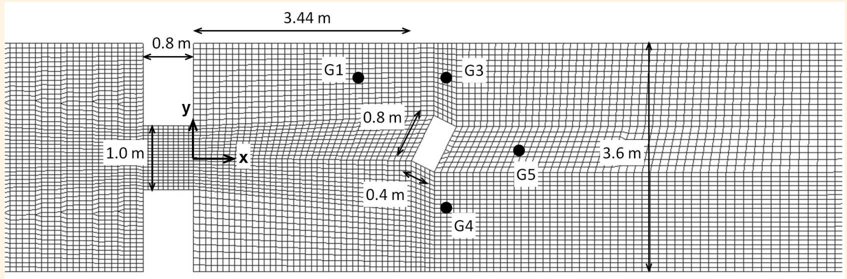

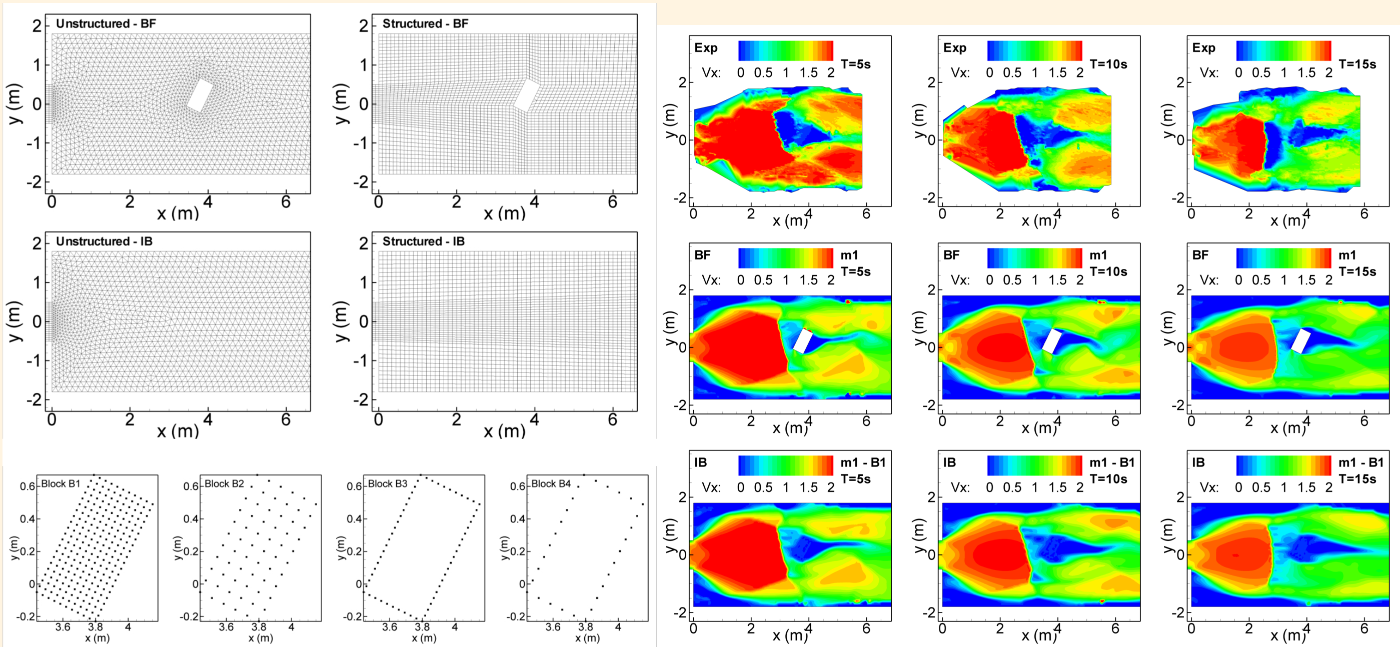

An immersed boundary method for unstructured meshes

01/38

Outline

- Introduction
- The FV-MLS method
- A MLS-based sliding mesh technique
- A High-order Chimera method
- An immersed boundary method for unstructured meshes
- Conclusions

Conclusions

- Many numerical applications using MLS with FV schemes have been presented.
- The accuracy and robustness of the new methodologies have been shown with different numerical test cases.
- MLS allows increasing the accuracy and capabilities of current FV codes.

A HIGH-ORDER CHIMERA METHOD BASED ON MOVING LEAST SQUARES APPROXIMATIONS

Luis Ramírez

email: luis.ramirez@udc.es

Thank you

—

Acknowledgments

- This work has been partially supported by:
  - The *Ministerio de Educación y Ciencia* of the Spanish Government,
  - *Dirección Xeral de I+D* of the *Consellería de Innovación, Industria e Comercio* of the *Xunta de Galicia*,
  - the *Universidade da Coruña (UDC)*, and
  - the *Group of Numerical Methods in Engineering - GMNI*

GOBIERNO DE ESPAÑA — MINISTERIO DE CIENCIA E INNOVACIÓN

UNIÓN EUROPEA — FONDO EUROPEO DE DESENVOLVEMENTO REXIONAL — "Unha maneira de facer Europa"

XUNTA DE GALICIA — CONSELLERÍA DE ECONOMÍA E INDUSTRIA

Some FV-MLS references

- L. Cueto-Felgueroso, I. Colominas, X. Nogueira, F. Navarrina, and M. Casteleiro, *Finite-volume solvers and moving least-squares approximations for the compressible Navier-Stokes equations on unstructured grids*, CMAME, 2007
- X. Nogueira, I. Colominas, L. Cueto-Felgueroso, and S. Khelladi, *On the simulation of wave propagation with a higher-order finite volume scheme based on reproducing kernel methods*, CMAME, 2010
- X. Nogueira, L. Cueto-Felgueroso, I. Colominas, F. Navarrina, and M. Casteleiro, *A new shock-capturing technique based on moving least squares for higher-order numerical schemes on unstructured grids*, CMAME, 2010
- X. Nogueira, L. Cueto-Felgueroso, I. Colominas, H.Gómez,*Implicit Large Eddy Simulation of non-wall-bounded turbulent flows based on the multiscale properties of a high-order finite volume method*, CMAME, 2010
- X. Nogueira, S. Khelladi, I. Colominas, L. Cueto-Felgueroso, J. París, and H. Gómez, *High-resolution finite volume methods on unstructured grids for turbulence and aeroacoustics*, ARCME, 2011
- S. Khelladi, X. Nogueira, F. Bakir, and I. Colominas, *Toward a higher-order unsteady finite volume solver based on reproducing kernel particle method*, CMAME, 2011.
- J.C. Chassaing, S. Khelladi, and X.Nogueira, *Accuracy assesment of a high-order moving least squares finite volume method for compressible flows*, C&F, 2013
- L. Ramirez, X. Nogueira, S. Khelladi, J.C. Chassaing, and I. Colominas, *A new higher-order finite volume method based on moving least squares for the resolution of the incompressible Navier-Stokes equations on unstructured grids*, CMAME, 2014